

Quantitative phase imaging of cells by Digital Holographic Microscopy

G.Hanu Phani Ram

A Dissertation Submitted to
Indian Institute of Technology Hyderabad
In Partial Fulfillment of the Requirements for
The Degree of Master of Technology



भारतीय प्रौद्योगिकी संस्थान हैदराबाद
Indian Institute of Technology Hyderabad

Department of Biomedical Engineering

June, 2014

Declaration

I declare that this written submission represents my ideas in my own words, and where others' ideas or words have been included, I have adequately cited and referenced the original sources. I also declare that I have adhered to all principles of academic honesty and integrity and have not misrepresented or fabricated or falsified any idea/data/fact/source in my submission. I understand that any violation of the above will be a cause for disciplinary action by the Institute and can also evoke penal action from the sources that have thus not been properly cited, or from whom proper permission has not been taken when needed.

Hanu

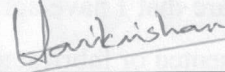
(Signature)

(G.Hanu Phani Ram)

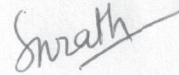
(BM12M1001)

Approval Sheet

This thesis entitled Quantitative Phase Imaging of cells by Digital Holographic Microscopy by G.Hanu Phani Ram is approved for the degree of Master of Technology from IIT Hyderabad.



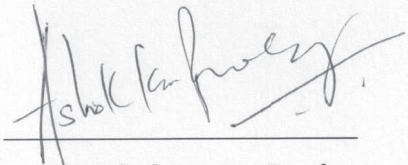
Dr. Harikrishnan Narayanan Unni
Assistant professor, Department of Biomedical Engineering
Indian Institute of Technology Hyderabad
Examiner



Dr. Subha Narayan Rath
Assistant professor, Department of Biomedical Engineering
Indian Institute of Technology Hyderabad
Examiner



Dr. Renu John
Assistant professor, Department of Biomedical Engineering
Indian Institute of Technology Hyderabad
Adviser



Dr. Ashok Kumar Pandey
Assistant professor, Department of Mechanical Engineering
Indian Institute of Technology Hyderabad
Chairman

Acknowledgements

I am very thankful to my supervisor Dr. Renu John, Department of Biomedical Engineering, IIT Hyderabad for his encouragement, valuable suggestions, and guidance throughout the project. Without his support I would have not reached this level. I am also thankful to Vimal Prabhu, PhD scholar for his help and suggestions.

I am thankful to all my friends for their support and family members for their support and care.

© 2014
Indian Institute of Technology, Hyderabad
India-502205

Dedicated to

To my parents

Abstract

We constructed digital holographic microscopy (DHM) setup for extracting the quantitative phase information of biological cells. Here we record the digital hologram of the object and perform computational reconstruction. The hologram recording is carried out on a CCD camera. CCD camera will digitize the information hence the method is known as ‘Digital Holographic Microscopy’. From the quantitative phase information, we can calculate the specimen (cell) thickness and volume. This method is advantageous compared to the existing techniques like bright field microscopy, phase contrast microscopy, differential interference contrast and other qualitative phase imaging techniques since they cannot give us exact phase information. In addition, this method is very attractive for live cell imaging as it does not require any contrast agents. In order to improve the resolution and field of view, the principle of Synthetic Apertures (SA) has been applied by moving the CCD camera to 9 positions and the acquired digital holograms were stitched together to increase the field of view with 22 Kilo pixels. We performed 3-D image reconstructions of a transparent ITO electrode. DHM being a quantitative phase imaging technique, could estimate the height and thickness of the ITO electrode. In order to show the improvement in resolution using synthetic apertures, we have imaged the USAF resolution chart. We have shown that the amplitude reconstruction of the USAF resolution chart has given better resolution in synthetic aperture digital holographic microscopy (SA-DHM) compared to DHM. We reconstructed 3 dimensional structure of an E.coli bacteria using SA-DHM and quantified its length and thickness.

Nomenclature

| | |
|------------------------------------------------|----------------------------------------------------------------------------------------|
| \emptyset | Phase angle |
| E_0 | light wave of object wave |
| E_R | light wave of reference wave |
| E_R^* | light wave of conjugate reference wave |
| H | hologram |
| $\Gamma(\acute{\epsilon}, \acute{\eta})$ | Reconstruction field |
| (ϵ, η) | co-ordinates in object plane |
| (x, y) | co-ordinates in hologram plane |
| $(\acute{\epsilon}, \acute{\eta})$ | co-ordinates in reconstruction plane |
| λ | Wavelength of light |
| ρ | Distance between a point in hologram plane to a point in reconstruction plane |
| d | Reconstruction distance from hologram plane to reconstruction plane |
| \mathfrak{F}_τ | Fresnel transformation operator |
| $\Delta x, \Delta y$ | pixel sizes in x and y direction in hologram plane |
| $\Delta \acute{\epsilon}, \Delta \acute{\eta}$ | pixel sizes in $\acute{\epsilon}$ and $\acute{\eta}$ direction in reconstruction plane |
| k_x, k_y | wave vector components in x and y-directions respectively. |
| D | radius of curvature which adjusts the curvature of the wave field |
| $P_{\alpha, \beta}$ | Polynomial coefficient of order $\alpha + \beta$ |
| Θ | convolution operator |
| $\Phi(\acute{\epsilon}, \acute{\eta})$ | Digital phase mask |
| DHM | Digital Holographic Microscopy |
| QPI | Quantitative Phase Imaging |
| SA-DHM | Synthetic Aperture-DHM |
| DPM | Digital Phase Mask |

List of figures

| | |
|----------------------------------------------------------------------------------------------------------|----|
| Figure 1-1 Amplitude and phase objects [16] | 8 |
| Figure 1-2 Microscopic objective [17] | 10 |
| Figure 1-3 Spherical aberration | 12 |
| Figure 1-4 Chromatic aberration | 12 |
| Figure 2-1 In line holography [29] | 19 |
| Figure 2-2 Reconstruction of in-line hologram [29]..... | 20 |
| Figure 2-3 Hologram recording [30]..... | 20 |
| Figure 2-4 Reconstruction of hologram[30] | 21 |
| Figure 2-5 Electronically recorded hologram [32]..... | 22 |
| Figure 2-6 computer reconstruction[32] | 22 |
| Figure 2-7 Reconstructed image[33]..... | 22 |
| Figure 2-8 Nondestructive testing by digital holographic interferometry [30]..... | 23 |
| Figure 2-9 Phase shifting digital holography[30]..... | 24 |
| Figure 2-10 DHM experimental setup, SF: spatial filter, S: sample, OBJ: microscopic objective [43]..... | 26 |
| Figure 3-1 Diffraction and interference [45]..... | 27 |
| Figure 3-2 Co-ordinate system of hologram formation and reconstruction..... | 29 |
| Figure 3-3 Wave front deformation by MO [44]..... | 34 |
| Figure 4-1 Experimental set-up for DHM | 37 |
| Figure 4-2 Hologram of letter 'H' | 38 |
| Figure 4-3 Amplitude reconstruction of letter H | 38 |
| Figure 4-4 Phase reconstruction of letter H | 39 |
| Figure 4-5 Recorded holograms for synthetic aperture reconstruction..... | 40 |
| Figure 4-6 mosaicked hologram..... | 41 |
| Figure 4-7 FFT of single hologram | 41 |
| Figure 4-8 FFT of synthetic aperture hologram..... | 42 |
| Figure 4-9 Filtered real image..... | 42 |
| Figure 4-10 Amplitude reconstruction without DPM | 43 |
| Figure 4-11 Phase reconstruction without DPM..... | 43 |
| Figure 4-12 Vertical profile | 43 |
| Figure 4-13 Horizontal profile | 44 |
| Figure 4-14 Reconstruction of single hologram | 44 |
| Figure 4-15 Reconstruction of synthetic aperture hologram..... | 45 |
| Figure 4-16 Surface plot of ITO electrode using synthetic aperture DHM | 45 |
| Figure 4-17 Amplitude reconstruction of synthetic aperture of USAF resolution chart..... | 46 |
| Figure 4-18 Amplitude reconstruction of single hologram of USAF resolution chart | 46 |
| Figure 4-19 Zoomed version of amplitude reconstruction synthetic hologram of USAF resolution chart | 46 |
| Figure 4-20 Zoomed version of amplitude reconstruction single hologram of USAF resolution chart | 46 |
| Figure 4-21 Phase reconstruction of E.coli | 47 |
| Figure 4-22 Multiplying E.Coli | 47 |
| Figure 4-23 E.coli reconstruction..... | 48 |

List of tables

| | |
|----------------------------------------------------------------|----|
| Table 1-1 Resolution of different microscopic objectives | 11 |
|----------------------------------------------------------------|----|

Contents

| | |
|------------------------------------------------------|------|
| Declaration..... | ii |
| Approval Sheet..... | iii |
| Acknowledgements..... | iv |
| Abstract..... | vii |
| Nomenclature | viii |
| List of figures | ix |
| List of tables | x |
| Chapter 1 | 1 |
| Introduction | 1 |
| 1.1. Bio-imaging..... | 1 |
| 1.1.1 History of bio-imaging..... | 4 |
| 1.1.2 Applications and scope of bio-imaging..... | 4 |
| 1.2. Microscopy for cell imaging..... | 5 |
| 1.3 Basics of optical microscopy..... | 8 |
| 1.3.1 Magnification..... | 9 |
| 1.3.2 Resolution..... | 9 |
| 1.3.3 Microscope objective..... | 10 |
| 1.3.4 Optical Aberrations..... | 11 |
| 1.4 Optical microscopic techniques..... | 13 |
| 1.5 Quantitative phase imaging (QPI) techniques..... | 15 |
| Chapter 2 | 18 |
| Optical and Digital Holography | 18 |
| 2.1 Introduction to holography..... | 18 |
| 2.1.1 Holography..... | 19 |
| 2.2 Digital Holographic Microscopy (DHM)..... | 21 |

| | |
|--------------------------------------------------------------|----|
| Chapter 3 | 27 |
| Principles of Digital Holographic Microscopy | 27 |
| 3.1 Basic principles of holography | 27 |
| 3.2 Mathematical formulation of digital holography | 28 |
| 3.2.1 Fresnel transformation method for reconstruction | 29 |
| 3.2.2 Convolution method for reconstruction | 31 |
| 3.4 Zero order diffraction and twin image elimination | 32 |
| 3.5 Aberration correction | 33 |
| Chapter 4 | 37 |
| Experiments and results | 37 |
| 4.1 Experimental setup | 37 |
| 4.2 Results | 37 |
| 4.2.1 Reconstruction of microscopic phase object | 39 |
| 4.2.2 Reconstruction of cells | 46 |
| Chapter 5 | 49 |
| Summary and future work | 49 |
| References | 50 |

Chapter 1

Introduction

1.1. Bio-imaging

Medical imaging is the visual representation of internal structure of the human body for the betterment of medical diagnosis and therapy. In olden days, anatomical structure of the body is found out by dissection as there were no proper noninvasive imaging techniques. At that time, physicians used to diagnose the problems in patients through physical observations and symptoms. The challenges in quick and accurate diagnosis of diseases have increased over time leading to the development of new diagnostic and therapeutic (thera-nostic) imaging modalities. The development of other technologies like micro and nanoelectronics, nanotechnology, high performance computing systems, software, enormous volumes of medical data and innovations in bio-imaging increased the research interests in the biomedical field, especially in biomedical imaging. Bio-imaging has revolutionized the clinical health sector. Its capabilities range from whole body to cellular down to the level of molecular imaging. Nowadays, through various biomedical imaging techniques, we can monitor the internal structure of human body non-invasively. The anatomy and physiology can also be studied and can differentiate the root cause for the abnormalities of unhealthy person using bio-imaging techniques, accordingly patients are treated.

Bio imaging started its journey with X-ray machine and it is still used everywhere because of its applications and non-invasive diagnosis. Even though X-rays have several advantages, it is harmful to the human body as prolonged exposure to it may induce cancer. Each modality uses particular energy waves, drugs or chemicals as a medium. Ultrasound uses sound waves as medium for imaging. Magnetic resonance imaging (MRI) uses strong magnetic field as medium. Positron emission tomography (PET) uses the principle of positron emission as source of imaging. These energy waves, optical energy, drugs, and contrast agents are used for imaging as these media have relationship with the type of tissue, or condition of the body. For example, optical imaging of biological cells depends on how the light interacts with the cell, the way the amplitude changes that depends upon the absorption properties of the cell and the way in which cell changes the phase of the light depends upon the cell thickness and the refractive index. So, the basis of bio-imaging is the interaction of biological tissues with energy waves or any other medium. The basic properties of interaction of energy fields with tissues are absorption, scattering, diffraction and interference. Based on the properties of the tissue, the interaction is dependent and the variations in the properties of energy fields

can either be observed directly by human eye or detectors are required so that they will map these detected fields onto the computer monitor for analyses.

After the invention of microscopy, focus is shifted more onto molecular and cellular bio-imaging. Cell is starting point for development of new therapeutics and complete understanding of its processes and intracellular interactions is necessary for whole organism pathways. Thus, scientists are trying to understand the complete cellular sub-structure and interactions, as cells are the basic units of living organisms. Techniques like histopathology are still gold standards for diagnostic purposes, though are very time consuming and carried out on ex vivo tissues. So, in vivo and live cell techniques are required to study the working of the cellular structures clearly. With the development of new drugs and probes, molecular imaging reached a new level. Scientists are working on molecular imaging as a new platform for testing and development of new drugs and theranostic probes. Many imaging modalities like Micro-PET (positron emission technology), micro-CT (computed tomography) micro-SPECT (single-photon emission computed tomography), micro-MRI (magnetic resonance imaging) are available for the preclinical and clinical molecular imaging.

Optical imaging techniques have applications in molecular and cellular imaging. Lot of development in optical molecular imaging has occurred because of development of targeted bioluminescence probes, near infrared fluorochromes, activatable near infrared fluorochromes and red shifted fluorescent proteins[1]. Optical imaging has advantage that multiple probes can be used for multichannel imaging. Cells are transparent for the light and molecules that are present inside the cell are not distinguishable from one another if we image through light alone. Protein detection is also part of analyzing the biological processes. Some kind of marker is necessary for the detection of proteins. Fluorescent proteins or probes made protein identification possible. Thus, Fluorescence imaging is one technique which improves the contrast of the image and useful for biomedical applications. In other words, fluorescence techniques add color to the normal imaging techniques. Some more imaging techniques like fluorescence life time imaging microscopy (FLIM) and fluorescence resonance energy transfer (FRET) came into existence for studying the protein-protein interactions[2]. Nanoparticles are also used for imaging the subcellular components and they should be less toxic and biocompatibility which depends upon the concentration. Whenever the nanoparticles are targeted to a particular site, cells take them by different processes like clathrin-based mechanisms, or phagocytosis which depends on the type and size of the cell as well as the surface charge of the nanoparticle conjugate[3]. Thus, nanoparticles are used for live or fixed cell imaging. Similarly magnetic nanoparticles has unique properties and they act as the contrast agents for the magnetic resonance imaging (MRI)[4].

Thus bio-imaging has brought up innovations in anatomical imaging for structural studies, physiological imaging for understanding different functional mechanisms inside the body, molecular imaging for deep understanding of the physiological processes at cellular and molecular level to understand

cell-cell, protein-protein interactions. Thus bio-imaging has its applications from nanoscale to macroscale. The present research in bio-imaging is aimed at improving the quality, resolution, minimum error (maximum signal to noise ratio) of the images for higher accuracy. Researchers are working on the instrumentation aspect of devices for marketing imaging devices at low cost. In rural areas, for any device to be implemented its cost as well as diagnosis cost should be as minimum as possible. So, researchers are working on low cost devices. Point of care diagnostics bring easy diagnostics aiming at large group of people both urban and rural areas as they are low cost, easy to access as they are portable, easy to maintain. Aydogan Ozcan et.al developed the cytometer as point of care diagnostics device using lensless holographic technique [5]. They also demonstrated the fluorescence imaging of fluorescent micro-objects and labeled cells in large field of view and also developed the low cost fluorescent imaging device using the cell phone [6, 7].

Characterization of a particular parameter pertaining to the disease diagnostics is very important. In qualitative analysis, the clinicians or physicians are trained to analyze qualitative images for disease identification and staging of disease, which is accepted in present medical practice especially in rural areas and developing countries. Similarly, Computed tomography (CT) is used for characterization which gives both qualitative and quantitative data of the subject. Thus quantitative imaging gives more information and suitable for taking the proper clinical decisions. It gives more accurate results and need not depend completely on observers as models are being developed for detection of diseases. According to the Radiological Society of North America (RSNA), quantitative imaging is “the extraction of quantifiable features from medical images for the assessment of normal or the severity, degree of change, or status of a disease, injury, or chronic condition relative to normal. Quantitative imaging includes the development, standardization, and optimization of anatomical, functional, and molecular imaging acquisition protocols, data analyses, display methods, and reporting structures. These features permit the validation of accurately and precisely obtained image-derived metrics with anatomically and physiologically relevant parameters, including treatment response and outcome, and the use of such metrics in research and patient care.”[8].

Bio-imaging is also used in image-guided surgeries and radiotherapy. The main aim is to reduce the time gap between the procedure and acquisition of images so that the body is less exposed to the radiation. It is used to target the radiation at the region of interest using other imaging techniques as a support. General electric (GE) has developed an interventional MRI unit that assists the physicians in interventional procedures. GE also proposes image guided therapy that aims at using focused ultrasound to treat cancer. Focused ultrasound is used in hyperthermia applications in image-guided radiotherapy.

Thus, bio-imaging has completely revolutionized the medical field and health sector. Still a lot more research should be carried out for development of accurate, low cost, reliable, portable, easily accessible, productive devices for health care.

1.1.1 History of bio-imaging

The first imaging device that was invented to image the internal structure of the body is X-ray machine which came into existence after discovery of X-rays by Wilhelm Rontgen. The use of Ultrasound technology in medical field was started from the early 1940's with wide variety of applications. It has notable applications in obstetrics and cardiology[9]. The measurement of blood flow using ultrasound started from 1955. The first positron imaging device was developed in 1950 where device was tested on the brain to localize the tumor. Later the device was extended to tomographic mode. In 1970's Computed Tomography (CT) was invented by Godfrey Hounsfield. The first clinical CT was setup between 1974 and 1976 whose application was limited to the imaging of the head. In late 1970's Magnetic Resonance Imaging (MRI) came into existence which is of great importance in clinical as well as research tool. In 1982 Paul Luterbur who was a noble laureate predicted that MRI will be become a valuable imaging technique to the existing techniques[10] and prediction turn out to be a right one. Multimodality imaging took birth to extract more data/knowledge of the patient's condition, examples like PET +MRI, CT+MRI. In 21st century, imaging is not only used for diagnosis, it also used in image guided therapy.

1.1.2 Applications and scope of bio-imaging

The main application of the imaging in the medical field is for the diagnosis and aid in the treatment. X-ray imaging gives complete understanding of the bone structure and can depict the abnormalities that occur due to injuries and disease condition. Kidney stones, gall stones, bone fracture & displacement can be detected using X-rays. Chest ray was used as the diagnosis tool for tuberculosis. X-ray angiography is popular for its ability to detect blood vessels; contrast agent should be given to the patients in this procedure. Though it has good applications, X-rays are harmful when someone is exposed to it continuously. In 1904, Clarence Dally, assistant to Thomas Edison in X-ray research died because of the severe exposure to X-ray. Ultrasound has many applications in orthopedic and physiotherapy for the treatment of musculoskeletal pain. It is also used in obstetrics where the weight and size of the baby can be estimated by the ultrasound imaging. Ultrasound is also used to diagnose the heart by measuring the blood flow. Positron emission tomography (PET) has a lot of applications. Earliest applications is study of brain diseases. PET with fluorodeoxyglucose (FDG) is considered as the diagnosis tool in oncology for lung, breast, head and neck, esophagus, colorectal. It can act as tool to detect the cancer stage. It also found applications for non-malignant diseases like dementia, inflammation and infection. It has many applications in neurology like Alzheimer's disease where PET-FDG can differentiate Alzheimer's and dementia , Huntington's disease , Parkinson's disease , epilepsy [11]. It has applications in cardiology like assessment of myocardial blood

flow, evaluation of beta receptors in heart, used to quantify extent of heart disease. The major applications of CT are CT angiography, cardiac imaging, virtual endoscopy and high resolution imaging [12]. Magnetic resonance imaging (MRI) has wide range of applications in neurology, cardiology, cancer and soft tissue assessment. For many central nervous system diseases MRI is considered to be the better diagnostic tool. It can detect abnormalities in entire range of central nervous system like brain, brain stem and spinal cord. It has many applications in the field of head, neck, mediastinum and chest, cardiovascular system, breast, abdomen, pelvis and musculoskeletal system [13]. The hybrid PET/MRI technology has lot of applications in oncology where it can detect breast cancer, sarcoidosis lesions, kidney lesions, adrenal gland lesion, prostate cancer, head-neck cancer, ovarian, cervical cancer, pediatric oncology, liver imaging. Thus it is whole body imaging modality technique.

1.2. Microscopy for cell imaging

Microscope is a device that magnifies an object which cannot be seen by naked eye. Microscopic imaging techniques play an important role in biomedical research and have lot of potential applications. According to the microscopy society of America, "Microscopy refers to the study of objects that are too small to be easily viewed by the unaided human eye. Viewing objects that range in size from millimeters down to as small as nanometers has always been fascinating to people from all walks of life, and is currently also applicable to virtually every field of science and technology". It uses many types of illumination sources such as white light, laser light, ions, electron beam, X-rays and mechanical probes to produce images. The objects under the microscope can be directly visualized by human eye (example: compound microscope) or image information is mapped to computer which is indirect method of observing microscopic objects (example: atomic force microscope). Our eye is capable of distinguishing only the visible range of Electromagnetic spectrum. We cannot perceive other rays like ultraviolet and infrared rays. Eye can also identify the change in the intensities but it cannot identify the change in the phase of the light. So, our eye is not capable of observing different ranges and parameters of light. So, microscopic techniques make us capable of visualizing the micro-objects and understand different parameters of the objects under study. Usually the microscopy can be broadly classified into three types

- 1, optical microscope
- 2, electron microscope
- 3, scanning probe microscope

Optical microscopes use lenses to magnify the image and use light source to illuminate the object. The image formation depends on interaction of the light with the sample. This interaction can be absorption, scattering and the fluorescence. Absorption of the light depends upon the light wavelength and type of tissue. Absorption coefficient gives us information on how the intensity of light changes as light penetrates

through the tissue. Beer-lamberts law gives relationship between intensity of light and absorption coefficient with penetration depth. Beer Lamberts law is given by

$$I = I_0 e^{-\mu_a z} \quad (1.1)$$

Where I_0 initial intensity of light, μ_a is the absorption coefficient and z is the penetration depth. Thus, after passing light through the object depending upon the absorption coefficient the light intensity varies, this reduced light intensity give us information about the object. Optical microscopic techniques like bright field microscopy are based upon the absorption coefficient of the micro-object or micro-organism under study. Cells have weak absorption property, therefore they cannot be imaged properly under bright field microscopes. Scattering is one more property of tissue when incident with light. Biological tissues are either highly scattering or weakly scattering. Laser beam broadening occurs because of the scattering. Detection of bacterial cells by light scattering method is described by the Bilyy et.al[14]. Dark field microscope produce image with dark background and contrast appear because of light scatter from the sample. Sometimes when sample is illuminated with the band of light, sample observe light of particular wavelength and emit light of different wavelength. This property of the sample is known as fluorescence. The microscopy used in detection of fluorescence is known as the fluorescence microscopy. Microscopy is not only limited to absorption, scattering and fluorescence properties of light, phase can be used as parameter for imaging like in phase contrast microscopy, differential interference contrast(DIC) microscopy and polarization is one more parameter that can be used for imaging like in polarizing light microscopy, DIC microscopy also uses polarization property of the light. Some other examples of optical microscopy are stereo microscopes and digital microscopes. Stereo microscope setup have two separate optical paths with two objectives and eyepieces to provide different viewing angles to left and right eye so that it produces three dimensional visualization of the sample. It is similar to the binocular vision of our eye. Binocular vision is responsible for the 3 dimensional perspective of objects we observe. It is used for dissection of micro-objects, microsurgery, sorting, inspection and making of small circuit boards. Digital microscope uses the USB cable to connect microscopic system output to the computer for further analysis of the images. An optical microscopy can be either a transmission microscopy or reflection microscopy whose usage depends on the object.

The first electron microscope prototype was made in the year 1931 by German physicist Ernst Ruska and Max knoll, its magnification power was four hundred at that time and later in 1933, Ernst Ruska built the electron microscope whose resolution exceed the optical microscope resolution. Electron microscope uses the electron beam to illuminate the sample. Electron microscopes have higher resolution and magnification than the optical microscope. The greater resolution is because of the smaller wavelength

of the electron compared to the optical wavelengths. The electron microscope uses electron beam to create high magnified images. Transmission electron microscope is of 1st kind of electron microscope which is similar to the light microscope, only difference is source of illumination. Siemens made first commercial TEM in 1939. Scanning electron microscope (SEM) is the electron microscope which scan the sample surface, where electrons interact with surface which contains information about topology of surface, composition and electrical conductivity. Electron microscope has lot of biological applications because of its high resolving nature. Its resolution can go till 1 nm. Several micro-organisms, viruses, bacteria can be seen using electron microscopy. The internal structure and organelles of cells are clearly seen under electron microscope. Thus, the whole anatomy can be studied under electron microscopy. Some of the disadvantages of using the electron microscope in comparison to the light microscope are they are very expensive, sample preparation is very difficult procedure and takes lot of time, sample must be dry, moving sample cannot be imaged hence it should be fixed; hence live cell imaging is not possible, the images are only black and white, the energy of electron beam is very high and may harm the biological sample. Thus, optical microscope is advantageous compared to electron microscope, except resolution and magnification are limited in optical microscope. Optical microscope is best suitable for observing live cells. The present research in optical microscopes mainly concerns with the resolution and contrast improvement for better understanding of the live cells.

The scanning tunneling microscope (SPM) is the 1st microscope of this category which was developed by Gerd Binnig and Heinrich Rohrer in 1981. Later in 1986, Gerd Binnig, Quate, and Gerber invented atomic force microscope (AFM). The microscopic images are formed by the interaction of the tip of the cantilever beam with the surface of the sample. Based on the interaction between the tip of the beam and the sample computer gathers data for image formation. The resolution of the SPM is less than 1 nm. SPM have capability move front and back on surface of the atoms. The interaction between cantilever tip and sample can be mechanical force, electrostatic force, magnetic force, chemical interaction, van der waal force and capillary force. SPM has lot of biological applications. AFM can be used for cell analysis, both for fixed and live cells in physiological environment[15]. It is used to detect the cell morphology and topology. It can also find the surface details of the structural proteins. Thus, SPM have good resolution compared to optical microscopic techniques. They also have capability to manipulate the atoms. Some of the disadvantages of the scanning probe microscopy is that they will take lot of time for imaging, it is not good for lateral imaging and they may damage the cells while scanning. It is good in height measurements and finding out the elastic properties of cell.

These three microscopic techniques namely optical microscopy, electron microscopy and scanning probe microscopy has lot of biological applications and has own advantages and disadvantages. Live cell imaging is yet another challenging task. The imaging environment should be similar to the physiological

conditions so that we study the cells as if we are studying them directly inside human body. Live cell imaging is necessary as there will not be fixation artifacts, we can see sequential events in real time; calcium signaling, ion gradients, membrane potentials etc can be recorded. Live cell imaging is not possible in electron microscopy as the electron radiation damages the cells. Thus, using electron microscopies, cells are highly resolvable but not effective. Scanning probing microscopy can also go to the nanometer resolution but it cannot give proper lateral imaging/information, some scanning techniques can also damage the cells, moreover it can only give the morphology and topography of the sample and the process of scanning is time consuming.

Three parameters that are important for live cell imaging are sensitivity of detection, acquisition rate and specimen viability. Optical microscopic techniques are good for live cell imaging as it does not require any staining, unless we want more contrast in the sample, we use staining in the fluorescence microscopic techniques. Optical techniques are completely non-invasive and non-destructive. Optical microscope uses light which is radiation-free and will not damage the specimen. These microscopes can form images of different colors because of the visible spectrum and colors are seen as a result of staining of sample.

Amplitude objects are those which absorb light when, light is passed through them. They allow remaining light to pass through which is of less magnitude compared to incident light. Bright field microscope can be used to image amplitude objects. Phase objects are those which change the phase of the incident light. Human eye can detect the changes in the amplitude but it cannot detect the changes in the phase. Cells are considered as phase objects as their absorption of light is very less; only the phase of the light is varied. These phase variations are dependent on the refractive index and the thickness of the specimen. The first microscope that worked on the phase images is Zernike's phase contrast microscopy. Fig 1.1 shows how the amplitude and phase objects change light.

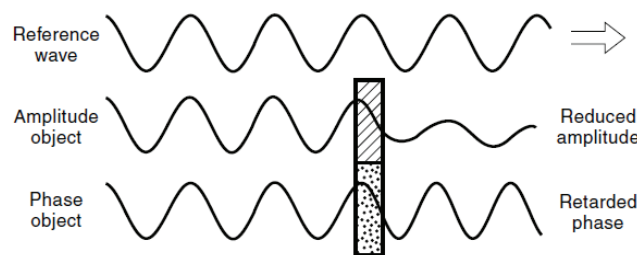


Figure 1-1 Amplitude and phase objects [16]

1.3 Basics of optical microscopy

Optical microscope use visible light and lenses to magnify the image. The conventional optical microscope has a single lens and the compound microscope uses multiple lenses. Though presently all

optical microscopes are compound microscopes, some magnifying devices have single lens. Magnification and resolution are the two important parameters to decide the application of any optical microscope.

1.3.1 Magnification

It gives the measure of the magnifying capability of the microscopic system. Magnification of system can be calculated by taking the ratio of size of an image to the size of the sample. Magnification is attained by using lenses. Magnification in the compound microscope is given by product of magnification of objective lens and magnification of eyepiece (ocular).

Total magnification of optical system = magnification of objective lens \times magnification of eyepiece

Increase in magnification of the sample beyond a particular limit would result in no further increase in resolution. This phenomenon is known as 'Empty magnification'. The image will be magnified but the resolution will not change if magnification cross this limit. The maximum magnification the light microscopes can go is 1500 times whereas the electron microscopes are capable to magnify up to 500000 times.

1.3.2 Resolution

Reason behind using a microscope is to see the samples clearly. Resolution is the most important parameter that decides the capability of a microscope. Resolution is the ability to distinguish two point objects that are close to each other. A normal eye can distinguish two point objects that are 0.1 millimeter apart, closer than that two point objects appear as single point object. Therefore, the resolving capability of our eye is 0.1 millimeter. Details of the image depend upon the resolution: Higher the resolution; greater the details. Resolution depends on the factors like wavelength of the incident light, refractive index of space between sample and Microscopic Objective front lens. It is given as

$$\text{Resolution } R = \frac{\text{wavelength}}{2 \times \text{numerical aperture}}$$

Numerical aperture (NA) = $n \times \sin \theta$, where n is refractive index of space between sample and MO front lens and θ is half of the angular objective aperture.

The ability to resolve is limited because of wavelengths in visible spectra (400-700 nm). The minimum wavelength in visible spectra is 400 nm. The oil immersion objectives can have the NA of 1 - 1.35. So, the maximum resolution can be from 150-200 nm. Thus, the resolution of the optical system is limited.

1.3.3 Microscope objective

Microscopic objective (MO) is the important part of the microscope as it decides the resolution of the image and the magnification of the sample. MO is placed right after the sample in the setup and closely as focal length of MO will be small and it will collect the rays diffracted from the sample. MO is most difficult component to design and fabricate as it is the combination of many micro-lenses. The modern microscopic objectives also do the aberration correction. While designing the MO manufacturers have to pay attention to the materials of lens and glass, refractive indices.

MO is selected for particular application based on the NA. NA decides the resolution apart from the wavelength of the light. The resolution will be improved by 1.5 times if we use immersion oil as the imaging medium rather than the air as medium. The magnification of the MO should be selected in such a way that the specimen should be clear. Fig 1.2 gives picture of MO

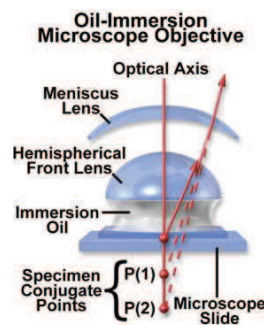


Figure 1-2 Microscopic objective [17]

Objectives that use water and/or glycerin as an imaging medium are also available for applications with living cells in culture of tissue immersed in saline solution[17]. Thus microscopic objective with digital holographic setup used as DHM. The resolution and magnification of the different microscopic objectives is given in table 1.

| Microscopic objective type | | | | | | |
|----------------------------|---------------|-----------------------------|---------------|-----------------------------|-----------------|-----------------------------|
| | Plan achromat | | plan fluorite | | plan apochromat | |
| Magnification | N.A | resolution(μm) | N.A | resolution(μm) | N.A | resolution(μm) |
| 4X | 0.1 | 2.75 | 0.13 | 2.12 | 0.2 | 1.375 |
| 10X | 0.25 | 1.1 | 0.3 | 0.92 | 0.45 | 0.61 |
| 20X | 0.4 | 0.69 | 0.5 | 0.55 | 0.75 | 0.37 |
| 40X | 0.65 | 0.42 | 0.75 | 0.37 | 0.95 | 0.29 |
| 60X | 0.75 | 0.37 | 0.85 | 0.32 | 0.95 | 0.29 |
| 100X | 1.25 | 0.22 | 1.3 | 0.21 | 1.40 | 0.2 |

Table 1-1 Resolution of different microscopic objectives

Source: www.microscopyu.com

1.3.4 Optical Aberrations

Aberrations are the errors that occur in the images because of imperfections in the lenses. Some aberrations are avoidable and some are not. The error in the images occur as wave field is varied with the aberrations. There are different types of aberrations, spherical aberration is one of aberrations that occur due to the geometry of the lenses. It occurs as shown in the Fig 1.3.

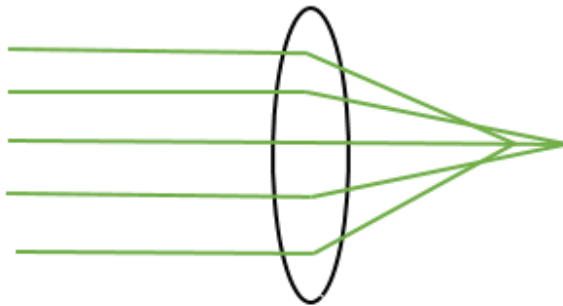


Figure 1-3 Spherical aberration

In spherical aberration, the rays near the paraxial region get focused at a different distance from the rays passing through the other parts of the lens. This aberration will degrade the image, clarity and sharpness of the image will be lost. Spherical aberration can be avoided by using the parabolic lenses where all the rays passing through the lens meet at the focus point. It can also be avoided by using additional lenses. Modern microscopes uses the special lens to avoid spherical aberration. One of the most common aberrations is chromatic aberration. Refractive index of the lens is function of wavelength, light of different wavelengths have different refractive index. Since white light contains visible spectrum, focal distance varies for each wavelength which result in chromatic aberration. Blue light will refract more than the green and red, therefore blue light has less focal length compare to green and red. The chromatic aberration is shown in Fig 1.4

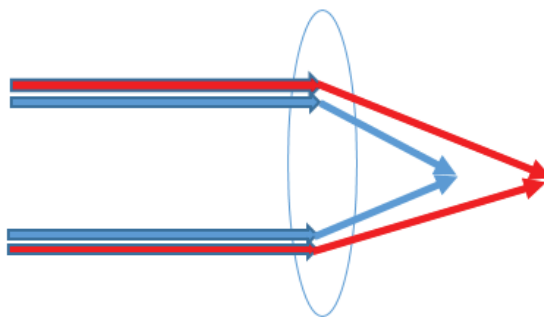


Figure 1-4 Chromatic aberration

Chromatic aberration can be minimized by using additional lenses. For example, achromatic lenses uses two lenses of different materials to cancel out the aberration.

Astigmatism is also one kind of aberration which occur when an optical system lacks cylindrical symmetry. The focus of rays varies in different directions due to asymmetrical lenses. Coma is another aberration which results in the off-axis rays from point of light to the focus. Coma can be partially corrected by tilting the lens. Field curvature aberration causes wave field curvature when a plane field is passed through the curved lens. Modern microscopes uses the flat field microscopic objectives to correct the field

curvature aberration. These are some of aberrations which can cause serious problems to the quality and clarity of the images. Modern day microscopic objectives are taking care of some aberrations. If any aberration occurs, it is always better to correct it to avoid image distortion.

1.4 Optical microscopic techniques

Optical microscopes are simplest microscopes. The history of microscopy started with the use of compound microscope by Robert Hooke to observe pores in cork which he called them as cells. Antoine van Leeuwenhoek is the first person to see the single celled organisms in pond water using the microscope. He used only single converging lens for magnification. In 1658, Jan Swammerdam observed erythrocytes with single lens microscopy. His main work was to observe the bodies of the insects at different stages of development. Marcello Malpighi observed brain, blood vessels, tongue, retina and development of chicken embryo. Johannes Evangelista Purkinje used the compound microscopy to discover purkinje neurons in cortex of cerebellum, sweat glands in skin, purkinje fibers in heart. In 1873, Abbe formulated limit for optical resolution related to the wavelength of the incident light and numerical aperture. Thus, many researchers started exploring the microscopes. Bright field microscopy is the simplest and the oldest microscopic technique where the dark contrast to the bright background will be obtained by absorption of the light by the sample. It can be used to observe fixed as well as live cells. As cells are transparent to the light staining is required to improve the contrast. The staining may result in artifacts. The resolution of the bright field microscope is limited to $0.2 \mu\text{m}$. So, bright field microscopy is best suitable for the amplitude objects. Phase objects cannot be seen properly in bright field microscopy. In Dark field microscope, bright sample is formed against the dark background. Here, a filter is used to remove the non-diffracted light, the image contains only the diffracted light. It is used to image bacteria, flagella, microtubules, actin filaments, unstained specimens. Thus, dark field microscope is good for light scattering specimens. Thus, bright field and dark field microscopic techniques are not good for phase objects like cells; phase information is utilized by Zernike for imaging using phase contrast microscopy. Thus phase changes are detected by Zernike with the invention of phase contrast microscopy in early 1930's. In phase contrast microscopy the phase information is converted to amplitude information. When light is incident upon the phase objects, zeroth order light passes through the specimen without deviation. Other wave is the diffracted wave, usually diffracted wave and non-diffracted wave has phase difference of $\lambda/4$. The diffracted light is delayed to non-diffracted light by $\lambda/4$. If a phase ring of phase delay $\lambda/4$ is introduced to the diffracted light then total phase delay between diffracted and non-diffracted light would be $\lambda/2$. Then they both interfere it would create a destructive interference which would make the sample dark with bright background. This is known as positive phase contrast. This is the principle for Zernike phase contrast microscopy. This method is not suitable for the thick specimens as thick materials appear distorted under phase contrast microscope. This

disadvantage is eliminated by the usage of differential interference contrast microscopy (DIC). DIC was made by Nomarski in early 1950's. In this technique, a polarizer is placed right after the light source. Polarizer converts unpolarized light into polarized light where the beam vibrate in particular direction. Then, a Wollaston prism is used to split the polarized light into two rays where one ray vibrate along the axis of the prism while other wave vibrate perpendicular to the 1st ray. One ray is allowed to pass through the specimen while other ray will act as background. Microscopic objective is placed after the specimen. 2nd Wollaston prism is placed after the objective which will bring two rays together. For the two rays to interfere they should vibrate in same plane and axis, therefore one more polarizer is used. The contrast depends upon thickness, refractive index of the object. When compared to the phase contrast microscopy DIC provides good resolution, good contrast and DIC can also be used for the thick specimens. For thickness calculation of the object, DIC is not preferable as it gives pseudo 3 dimensional view. For thin specimens phase contrast is preferable. All the techniques discussed above can be used without staining specimens. Sometimes, specimens are stained to have the better contrast and some specimens have intrinsic property where they emit light when they are exposed to particular bandwidth (wavelength range) of light. Fluorescence occurs when specimen absorb particular wavelength of the light and emit light of some other wavelength. This can be either property of the specimen or Fluorescence dyes. Fluorescent dyes are the contrast agents which increase the contrast of the specimen. Maximum excitation of the specimen occurs at region of maximal absorption. For example porphyrin which is naturally occurring contrast agent has maximum absorption at 400nm and 600 nm where the maximum emission occurs [18]. Also ultraviolet radiation can also excite many organic molecules. In bio imaging applications, contrast agents help biologists to observe specific locations. For example, Green fluorescent proteins (GFP) help to observe location of specific proteins in cell. Some other recent applications of fluorescent microscope are single molecule analysis of proteins, use of quantum dots to study single molecule in living cells, in vivo tracking of immune cells using fluorescence labels [19].

Disadvantage of using fluorescence microscopy is the usage of fluorescent dyes as they can be toxic to the living specimens. One of the useful imaging technique in biomedical imaging is confocal microscopy. It was first proposed by Nipkow and later developed by a Harvard post-doc fellow Minsky in 1957. In a fluorescence imaging fluorescence emission happen from the complete thickness of the specimen.so, the image contain the out of focus information. In confocal microscopy, only in focus point (ideal) information is utilized for imaging by using spatial filter which would eliminate the out of focus information. The resolution of the image in this microscopy is improved compared to the standard microscopy. Horizontal scanning is performed to obtain stacks of data and using algorithms, three dimensional structure of the sample is reconstructed. Confocal microscopy can be used for live cell imaging. Proteins of interest can be tracked by tagging them to green fluorescent proteins or others tags. It is also

used to analyze the subcellular functions such as pH gradients and membrane potentials. It is also used to measure the ionic concentration changes inside the cell.

Most of optical imaging techniques that we have discussed so far are the qualitative imaging techniques. Here we cannot calculate the thickness, volume and refractive index of the specimen. We saw how the phase is converted to amplitude in phase contrast microscopy. Qualitative phase imaging techniques are useful in characterizing the specimens where phase values are calculated which in turn are used to calculate different parameters.

1.5 Quantitative phase imaging (QPI) techniques

Qualitative phase imaging techniques are used only for observational and imaging purpose and these techniques convert phase variations to amplitude variations to provide contrast between sample and background, whereas quantitative phase imaging techniques help us to calculate exact phase shift due to the sample. This phase information is used for the calculation of several parameters like refractive index, thickness and volume of the sample. It has lot of biomedical applications. There are many quantitative phase imaging techniques like Hilbert phase microscopy (HPM), Optical quadrature microscopy, Fourier phase microscopy, diffraction phase microscopy, white light diffraction phase microscopy, spatial light interference microscopy, instantaneous spatial light interference microscopy, QPI using transport of intensity and digital holographic microscopy. Hilbert phase microscopy is an off-axis quantitative phase imaging technique. This is an interferometric set-up where an interferogram is recorded in the image plane and only one interferogram recording is required. So, the acquisition time is limited only by the recording device. Thus HPM is used for nanoscale measurements with acquisition rate of milliseconds and therefore useful in quantifying cytoskeletal dynamics, cell membrane fluctuations and neural activity as these processes occur in millisecond range [20]. Some other applications of HPM are live cell imaging, studying red blood cells morphology [21]. Optical quadrature microscopy (OQM) is phase shift based QPI technique. OQM consists of phase shifting mach-zehnder interferometer with polarizers and four CCD cameras to receive data simultaneously. Phase information is calculated from those data. Multimodal imaging is possible along with differential interference contrast microscopy [22]. Some applications of OQM are counting the number of cells in embryos. It is also used for the detection of the viability of mouse embryos [23]. Fourier phase microscopy (FPM) is common path quantitative phase imaging technique where interference occurs between the uniform fields and spatially varying field. Programmable phase modulator (PPM) is used to change the phase of the spatially varying field component with respect to the uniform field [24] and 4 interference images are recorded with phase difference of 0 , $\pi/2$, π , and $3\pi/2$. From these 4 recorded interferograms, phase can be calculated. FPM is used for live cell imaging and measure nanoscale fluctuations of erythrocytes from few seconds to several hours. FPM is also used for the measurement of

the cell growth. Diffraction phase microscopy (DPM) is quantitative phase imaging technique which combines the benefits of HPM single shot interferogram and common path geometry of the FPM [25]. Thus, it provides fast phase images. In the experimental set up of DPM, a plane beam is passed through the sample and collimate the beam, then grating is used to separate 0th and 1st order of sample beam and Mach-Zehnder common path interferometer is made and 0th and 1st order beams act as the reference and object beam respectively to interfere at the CCD plane. For the 0th order to act as a reference, it should passed through pin hole to remove the high frequencies. DPM is used along with the fluorescence microscopy so that both structural as well as functional information can be known. Some applications of the DPM are live red cell imaging, neuron cell imaging, red blood cell mechanics, imaging of malaria infected red blood cells [26]. DPM is also used for imaging the kidney cells in the culture. White light diffraction phase microscopy (wDPM) is similar to the DPM except illumination source in DPM is laser whereas the source in wDPM is spatially coherent white source. The usage of white light reduces the speckle noise. Here 0th and 1st order beams are allowed to interfere to produce interference fringes that are recorded by the CCD camera. wDPM is used for live red blood cell imaging and measurement of the cell growth over long period of time [27]. It also has applications in RBC membrane fluctuation measurement, quantitative phase imaging of beating cardiomyocyte cell [14]. Instantaneous spatial light interference microscopy (iSLIM) is a quantitative phase method which combines the benefits of the white light phase contrast microscopy and phase stability resulted from the diffraction phase microscopy [28]. It has significant advantages as it won't have speckle noise due to white light illumination, add-on capability to the available phase contrast microscopy, phase stability due to the common path geometry of the DPM. Some of its applications are measurement of cell fluctuations, measure mechanical properties of the cell. One of quantitative imaging method transport of intensity equation (TIE) where is no specific setup for imaging rather the phase information is hidden in the image field. The phase can be calculated by transport of intensity equation. Here the intensity images of the out of focus plane are recorded and using those images phase information of the in focus field can be calculated. Using TIE cell imaging can be performed, measurement of the live cell, study the red blood cell variations. The main advantage of TIE is that we can perform the quantitative imaging without a need of extra optical setup. Standard optical microscope is sufficient for the QPI analysis using TIE. Digital holographic microscopy is also one of the quantitative phase imaging technique.

Digital Holographic Microscopy (DHM) is used for extracting the quantitative phase information of biological cells. Here we record the digital hologram of the object and perform computational reconstruction. The hologram recording is done on a CCD camera. CCD camera will digitize the information hence the method is known as 'Digital Holographic Microscopy'. From the quantitative phase information we can calculate the specimen (cell) thickness and refractive index. This method is advantageous to the existing techniques like bright field microscopy, phase contrast microscopy,

differential interference contrast and other qualitative phase imaging techniques since they cannot give us exact phase information. In addition, this method is very attractive for live cell imaging as it does not require any contrast agents.

Chapter 2

Optical and Digital Holography

2.1 Introduction to holography

In 1940's Dennis Gabor, a British scientist found out the principle of holography while he was working to improve the resolution of electron microscopy. The further developments in the field of holography is hindered because of the unavailability of proper light source with property like coherence. For holographic techniques coherence is an important property for interference to occur. The development of holographic imaging started with the invention of laser, which was invented by Russian scientists N. Bassov and A. Prokhorov and American scientist Charles towns in 1960's. In 1962, Leith and Upatneiks used laser and off-axis method which they adopted from their previous work to develop holographic techniques to image 3D objects. That was the first laser transmission hologram of 3D objects. The holographic off-axis technique which Leith and Upatneiks developed is still use as standard holographic technique for various applications. In 1962, Russian scientist Dr. Yuri N Denisyuk combined holographic technique and natural color photographic technique to produce white light reflection hologram. In 1965, Powell and Stetson published first article on holographic interferometry (HI). HI is used as a technique to test the deformations of the objects. In 1967, shankoff and Pennigton bi-chrome gelatin as the material for recording the holograms. Thus, holograms are recorded on the clear, non-porous bi-chrome gelatin film. In 1971, Dennis Gabor received noble prize in physics for his invention of holography. In 1972, Lloyd cross combined white light transmission holography and conventional cinematography to produce integral holograms to reconstruct moving 3D images. In 1972, Tung Jeong started offering summer classes on holography at Lake Forest College to instruct educators on how to teach holography. In 1983, Master card international became first company to use hologram for bank card security and national geographic magazine was first major publication to use hologram on its cover. Holography became an important research field as it has many applications. Some of the recent applications of holography are digital holographic microscopy, incoherent holography, x-ray holography, holographic television, and holographic tweezers.

2.1.1 Holography

Holography is an optical imaging technique where a 3 dimensional image is recorded on photographic film and reconstructed. The recorded optical pattern on the photographic plate is known as the hologram. The word hologram is taken from the Greek word where holos means whole and gramma means message. Thus, hologram contains information of the whole 3 dimensional object in the 2 dimensional hologram which is recorded on the photographic plate. Holography is an interferometry technique where a two beam of rays interfere on the hologram plane, one beam is known as object beam which is diffracted from the object and 2nd beam is known as reference beam. Thus, both beams interfere at the photographic film. The recorded pattern is known as the hologram.

Gabor invented a new microscopic technique. The technique which he developed is known as in-line holography as object wave and reference wave have common path.

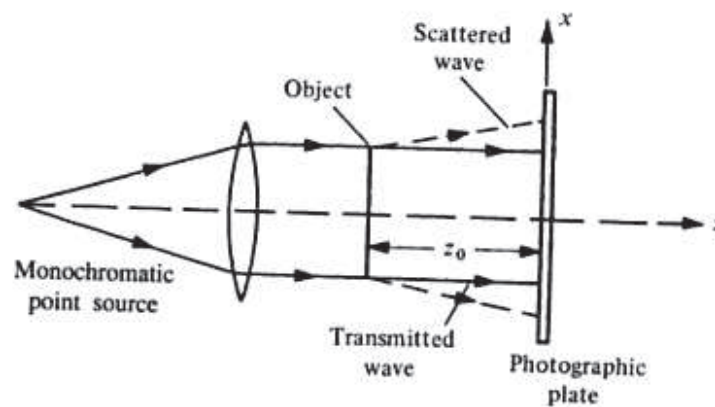


Figure 2-1 In line holography [29]

In-line holography as shown in Fig 2.1, a monochromatic point source is used and followed by collimator and beam of light is incident on the object which scatters the light. This scattered wave field act as the object beam and the 0th order undeviated wave will act as the reference beam. Thus, object and reference beam will interfere at the photographic plate.

The object is reconstructed by illumination of the source onto the hologram as shown in the Fig 2.2. When light is incident on hologram two images are formed, one is

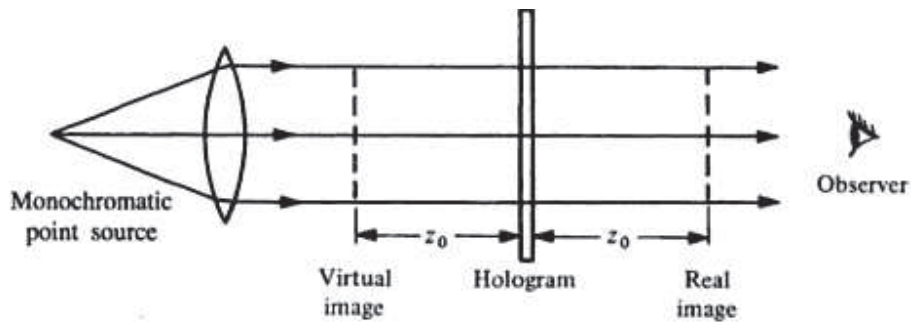


Figure 2-2 Reconstruction of in-line hologram [29]

real image and other one is a virtual image. In inline setup, the reconstructed real image is superimposed by the undeviated part and the virtual image lie on same optical axis. This can be avoided by the use of off-axis setup.

In off-axis hologram, object beam and reference beam will interfere at particular angle $\Theta \neq 0$ degree.

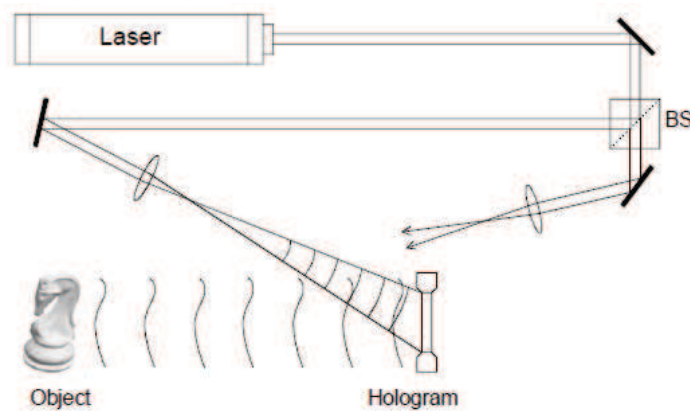


Figure 2-3 Hologram recording [30]

Formation of off-axis holography is similar to the Gabor's in-line holography. The alignment in recording the hologram is Mach-zehnder interferometer. Laser is used as the source. We can observe from the above Fig 2.3 how hologram is recorded. It is recorded by the interference of object beam and reference beam. Object beam is the wave field that is scattered from the object whereas the reference beam is the laser wave field which is not altered. Thus, the interference pattern is formed on the photographic plate which is known as hologram.

The reconstruction procedure is same as that of the in-line holography. Reference wave is incident on the hologram to reconstruct the object. An observer can see the virtual image with its 3 dimensional perspective as shown in the Fig 2.4

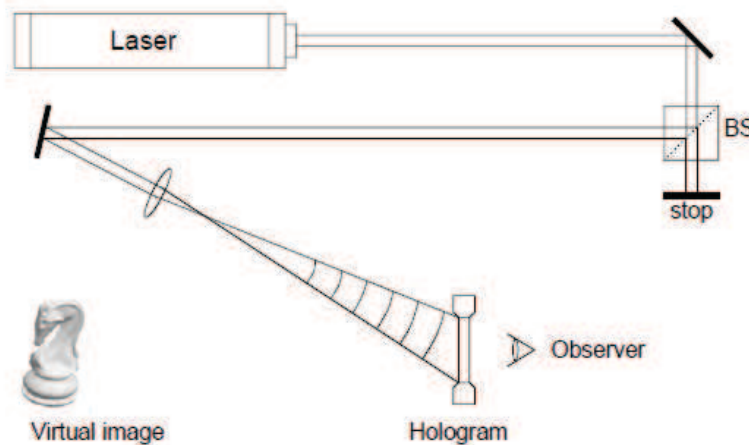


Figure 2-4 Reconstruction of hologram[30]

Whatever we discussed so far is related to the optical holography. Which mean the recording and reconstruction of the object wave field is carried out optically. One of the disadvantage of using the optical holography is the reconstructed object can only be seen by its depth but cannot characterize it quantitatively. This can be eliminated by using the digital holography which is explained in the next section.

2.2 Digital Holographic Microscopy (DHM)

The origin of digital holography started with the work of 'computer generated holograms (CGH)' where holograms are generated computationally and reconstructed the object optically. CGH was first started by B. R .Brown and A. W. Lohmann[31]. They used the computer guided plotter to draw the hologram which contains only the binary transmittance values. The quality of reconstruction of the hologram generated computationally is as good as reconstruction of the optically generated holograms. CGH will reduce the hardware that is required for the hologram generation. The numerical reconstruction of the holograms was started by J. W. Goodman and R. W. Lawrence [32]. The first step of recording is same as that of the Gabor's except that the optical recording is converted to the digital data and computer is used to reconstruct the object numerically. This method has advantage as it can able to detect objects of small angular sub-tense[32]. Here, the hologram is recorded on the photosensitive material and optically

recorded hologram is sampled to convert into the digitized form which is then reconstructed computationally.

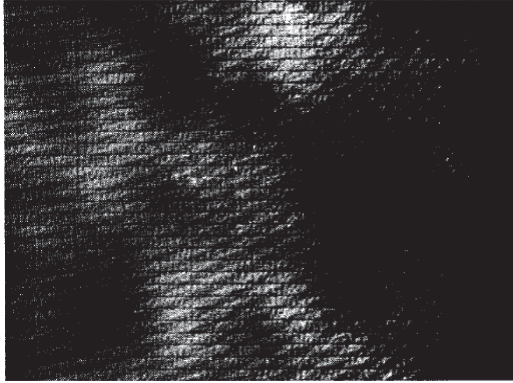


Figure 2-5 Electronically recorded hologram [32]

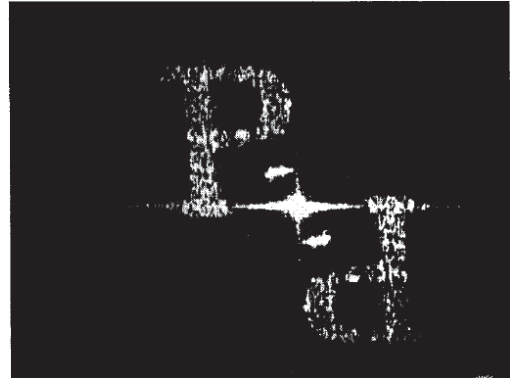


Figure 2-6 computer reconstruction[32]

In Fig 2.5, computer recorded hologram of the transparent P object and the computer reconstruction of the object is shown in the Fig 2.6. Later several researchers worked on mathematical modelling for reconstruction of the optical wave field of the object and also they worked on developing the algorithms.

The invention of charge coupled devices (CCD) has brought up lot of changes in digital holography. In the place of photosensitive material, the use of CCD avoid the usage of chemicals. U. Schnars and W. Juptner[33] described the direct recording of the hologram with the usage of CCD and reconstruction of the object. They demonstrated the off-axis hologram of a die and its reconstruction, the plane reference beam and the scattered object beam from the object beam are interfered on the CCD at certain angle which can be at maximum of few degrees. The reconstructed image which they have shown is given in the Fig 2.7 has both undiffracted wave field as well as the object die which are separated from each other due to the off-axis setup. Also speckles are seen, which are formed when there is interaction between coherent light and the rough surface.

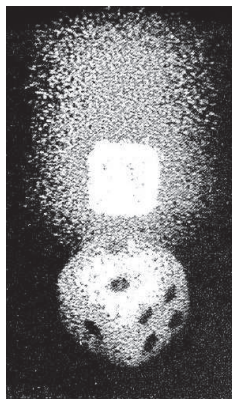


Figure 2-7 Reconstructed image[33]

Thus, CCD is well suited for the numerical reconstruction of the objects. CCDs have more sensitivity

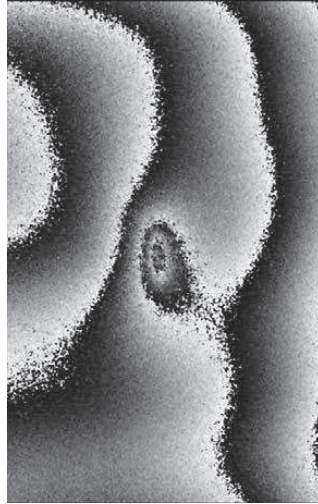


Figure 2-8 Nondestructive testing by digital holographic interferometry [30]

and resolution compared to the photographic film. Thus, quality of the images are improved using CCD. This method of reconstruction of the object recorded digitally is known as the ‘Digital holography’. The whole optical wave field of the object can be reconstruction by mathematical modelling of the light propagation using the properties like interference and diffraction which are the basis for holography. Formulation of mathematical equations help in depicting the wave field pattern of the object The main application of digital holography is quantitative phase imaging technique where we can calculate exact thickness, volume and refractive index of the object. Cucho et.al[34] explained the simultaneous amplitude and phase reconstruction of the object and this method gives the surface profile of the object. Usually the phase values are calculated along the surface and it is converted to the height of the specimen. Digital holography is used in the shape, deformation measurement and ultimately used to completely characterize the object. The beauty of digital holographic techniques is that it is non-invasive, therefore non-destructive for testing the materials and this feature suit for deformation measurements. Nondestructive testing has applications in science, industry and it is also used in electrical, mechanical, forensic, civil, aeronautical engineering and medicine. Some of Holographic nondestructive testing methods are holographic interferometry (HI), electronic speckle pattern interferometry(ESPI) and shearography. The deformation in the materials can be seen and calculated from the fringe pattern. Quantitative measurement is sometimes not required to find out defects in sample. Just by analyzing the interference pattern one can find out flaws in the object qualitatively. In Fig 2.8 it can be seen that the disturbance in the fringe pattern can identify the flaw.

These testing methods can also measure the deformation due to thermal and mechanical loading of the object under study. Holographic nondestructive testing can measure deformations in range of sub micrometer range. Simultaneous in-plane and out of plane deformations can be measured using digital holography which was explained by G. Pedrini[35]. This concept of digital holography is extended to digital holographic interferometry and shearography by U. Schnars and W. Juptner [36] in 1994. In digital holographic interferometry, hologram of the object is recorded in two different conditions and these two holograms are interfered to form interferogram. This is similar to the hologram interferometry where two object waves are recorded to form interferogram. Two hologram recording in different condition is carried out optically but superposition of two holograms to form interferogram is computational. For the reconstruction of the object Fresnel transformation can be used, where superimposed hologram is multiplied with the reference beam and product is Fresnel propagated to the image plane. The mathematical formulation will be explained in the **Chapter 3**. The direct phase calculation in hologram interferometry was explained by U Schnars [37]. Some applications of Digital HI are deformation and shape measurement , calculation of mechanical and thermal properties such as Young’s modulus, Poisson’s ratio and thermal expansion coefficients, nondestructive testing In shearography, reconstructed object wave amplitude field shifted laterally and that shifted field is superimposed with the original object wave field. Phase shifting digital holography [38] is technique where complex amplitude is measured at a plane. It is a two beam interferometer technique where one beam is object beam which is either scattered or diffracted depending upon the specimen and 2nd beam is passed through the piezoelectric transducer mirror which will phase shift the beam. The both beams interfere and interference pattern is recorded on CCD as shown in the Fig 2.9.

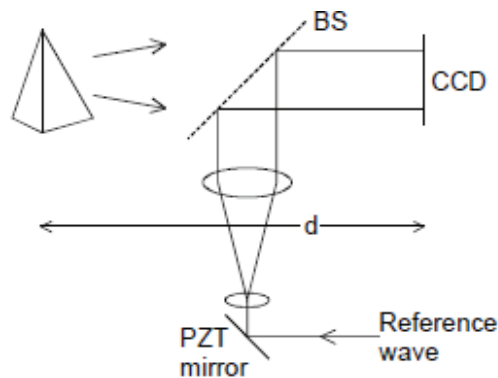


Figure 2-9 Phase shifting digital holography[30]

The complex amplitude object wave field reconstruction at particular plane is obtained computationally and image is reconstructed. Thus, this method is gives the 3 dimensional view of the object of good quality, gives wider image field and greater resolution compared to off-axis digital holography setup. Using this method the quantitative information of the object and deformation of the 3D objects can

be extracted using numerical methods. Songcan Lie et.al proposed a phase shift inline digital holography[39] for reconstruction of the complete wave field of the object. The main challenge in inline holography would be to eliminate the conjugate image. In this method four holograms are recorded with changing the phase values of reference beam. Algorithms are used to get back the object wave field. Surface contouring and shape measurements can be calculated by the phase shifting digital holography as explained by Yamaguchi et al[40]. It gives amplitude and phase information and images. Many digital holographic methods are limited to the single wavelength whereas phase shifting color digital holography as explained Yamaguchi et.al[41] use multiple wavelengths. The main application of this method is to reconstruct the colored object using multi-wavelength laser source and CCD camera. The optical set up is similar to that of the phase shifting digital holography and the interference pattern for the each wavelength is recorded simultaneously by the colored CCD camera. This method can also be used for analysis of the biological samples where they are stained with chemicals. Some other applications of the digital holography is in securing the information as explained by Javidi et.al [42]. The encrypted image is stored as the digital hologram and this data can be transmitted as well as decrypted digitally. Not only 2D information but the 3D information can be encrypted using digital holography. Thus, digital holographic methods have lot applications in many fields like optical metrology, biomedical, security and various other fields. The success of digital holography lies in its ability to calculate the different parameters of the object without touching the object, no staining of the objects is required, and the whole 3 dimensional information just lies in the 2 dimensional hologram. Single recording of the object is enough in digital holography for reconstruction of object which make this imaging technique fast. The usage of CCD camera makes even more efficient and faster. Lot of analysis and calculation of the wave field is carried out after recording the hologram as later part is computational which avoids the optical setup for the reconstruction. It has many applications as ‘Digital holographic microscopy’.

Gabor invented holography which he was working with the lens less electron microscopy technique but holographic technique is now applied to the microscopy and it can deliver better images compared to the standard microscopic techniques. It can also give the quantitative information of the micro scale objects as explained in Digital holography.

DHM is the combination of the digital holography with the microscopy technique. Digital holography uses CCD as a recording medium for the optical holography. DHM setup require microscopic objective as an additional component to the digital holographic setup. We will discuss in more detail about the experimental setup later in **Chapter 4**. The experimental setup of DHM is shown in figure 2.10

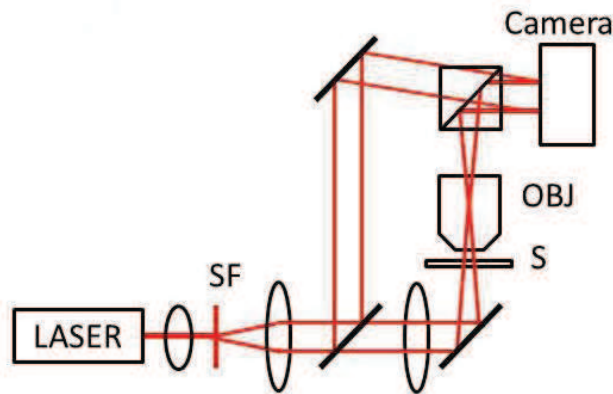


Figure 2-10 DHM experimental setup, SF: spatial filter, S: sample, OBJ: microscopic objective [43]

In DHM, a laser beam is used as a source of light as light should be coherent for interference to happen, spatial filter is used to clean the beam, then using the beam splitter the beam will be divided into two arms, one is the reference beam where a plane beam will reach the CCD and 2nd arm is the object arm where the beam is incident on the sample the wave field is collected by the microscopic objective which will magnify the sample. Thus the reference beam and magnified object beam interfere on the CCD. Reconstruction is numerically performed in a computer. Thus, DHM is used as the microscopic imaging technique which can image micro scale objects. DHM is simultaneous amplitude and quantitative phase contrast microscopy as explained by Cucho et.al [44]

DHM has applications in many fields as it is non-invasive, non-destructive and gives the full field quantitative information, its applications are the extension of the digital holographic applications but at the micro level and. It is used in optical metrology, device inspection, MEMS characterization etc. and. MEMS devices will be in range of micrometer and as size decreases the complexity of devices increases and testing them is necessary. DHM is used as testing tool for MEMS characterization. DHM can give static as well as the dynamic characterization of MEMS devices. It can also detect the out of plane deformation that occur as a result of the residual stress. The variations of the device due to external factors like temperature, pressure, electrostatic can be detected using DHM. It also has biological applications like live cell imaging, nerve cell imaging, and volumetric cell imaging which can be used as the diagnostic device. Quantitative phase imaging is carried out by DHM where phase map of live cells are obtained and we can calculate the cell thickness, cellular refractive index and the 3 dimensional structure of the cells. Thus DHM has wide applications in optical metrology, life sciences.

Chapter 3

Principles of Digital Holographic Microscopy

3.1 Basic principles of holography

Light wave can be either wave nature or particle nature. Holography is based upon the wave nature of light, where Interference and diffraction are the basis for holography. The concept of holography was clearly demonstrated by Thomas young in his double slit experiment. He used a screen with two holes and allowed sunrays to pass through it and he observed a series of light and dark bands on the white screen which was kept in front of the screen with two pin hole. This phenomenon is known as the interference. It occurs because of superposition of two waves. Thus, the superposition can be either constructive or destructive depending on the phase difference between two waves. Thus, constructive and destructive interference decides dark and light bands. Constructive interference gives light band and destructive interference gives dark band. For interference to occur two light waves should be coherent. Coherence is the property of light waves which maintains constant phase difference. Interference between object wave and reference wave occurs in hologram plane resulting in hologram formation. Whenever light passes through the opaque object, shadow doesn't form as predict by geometrical optics, this is because of property called diffraction which occur as a result of bending of the light waves at the edges or transparent holes in the object. The bending of light waves at the corner of slit depends upon its size. In young's double slit experiment both diffraction and interference occurs as shown in the figure 3.1.

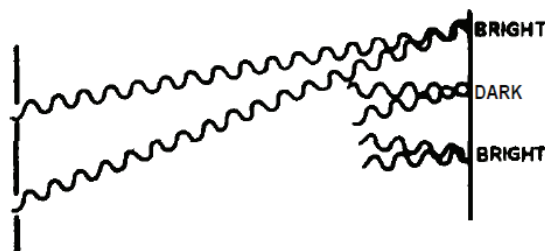


Figure 3-1 Diffraction and interference [45]

3.2 Mathematical formulation of digital holography

Any three dimensional wave which is having amplitude a and phase \emptyset is given by

$$E(x, y) = a(x, y)\exp(i\emptyset(x, y)) \quad (3.1)$$

Therefore, let the object wave and reference waves are given by equations (3.2) and (3.3) respectively

$$E_o(x, y) = a_o(x, y)\exp(i\emptyset_o(x, y)) \quad (3.2)$$

$$E_R(x, y) = a_R(x, y)\exp(i\emptyset_R(x, y)) \quad (3.3)$$

The object and reference waves interfere at the hologram plane, usually the recording medium, here CCD will record the intensity of the superimposed waves.

Therefore, hologram = intensity of superimposed waves

$$\begin{aligned} H(x, y) &= |E_o + E_R|^2 \\ &= |E_o|^2 + |E_R|^2 + E_o \cdot E_R^* + E_o^* \cdot E_R \end{aligned} \quad (3.4)$$

The reconstruction of the object is explained in section 2.1.2 where the recorded hologram is incident with the reference wave. As digital holography reconstruction is carried numerically, we multiply hologram $H(x, y)$ with conjugate of reference wave E_R^* , as multiplying reference wave E_R will result in the distortion of the real image as explained in [30]. Therefore reconstruction of hologram is given in equation (3.5).

$$\begin{aligned} \text{Reference conj. } (E_R^*(x, y)) * \text{hologram } H(x, y) \\ &= E_R^*(x, y) \cdot H(x, y) \\ &= E_R^*(x, y) \cdot (|E_o|^2 + |E_R|^2 + E_o \cdot E_R^* + E_o^* \cdot E_R) \\ &= E_R^*(x, y) \cdot (|E_o|^2 + |E_R|^2) + E_o \cdot (E_R^*)^2 + E_o^* \cdot |E_R|^2 \end{aligned} \quad (3.5)$$

We can observe that there are three terms in the numerically reconstructed object. The first term represents conjugate reference term multiplied with a constant factor which represents zeroth order term which is non-diffracted wave passing through the hologram. The second term represents virtual image which is distorted by the term $(E_R^*)^2$. The third term represents the real image which is multiplied with intensity of reference wave. Thus, the numerically reconstructed wave field contains the zeroth order term, distorted virtual image and a real image.

3.2.1 Fresnel transformation method for reconstruction

In order to reconstruct the wave field we need to understand the diffraction of wave field in the hologram plane which is explained by Fresnel Kirchhoff integral[30] as given in equation 3.6 below with respect to co-ordinate system shown in Fig 3.2.

$$\Gamma(\xi, \eta) = \frac{i}{\lambda} \iint_{-\infty}^{+\infty} H(x, y) E_R^*(x, y) \frac{\exp(-i\frac{2\pi}{\lambda}\rho)}{\rho} dx dy \quad (3.6)$$

$\Gamma(\xi, \eta)$ is wave-field reconstruction in the image plane, λ is wavelength of the light. $H(x, y)$ and $E_R^*(x, y)$ are the hologram and conjugate reference beam respectively. The hologram is considered to be aperture. When Reference is incident on the hologram, the wave field in the observation plane is dependent on hologram and $\frac{\exp(-i\frac{2\pi}{\lambda}\rho)}{\rho}$ represents the secondary spherical waves that are emanating from a single aperture, therefore the complete wave-field in the reconstruction plane is integral over all the secondary spherical waves. Thus reconstruction wave-field is given in equation 3.6 known as ‘Fresnel Kirchhoff integral’. ρ is distance between a point in hologram plane to a point in reconstruction plane given in equation (3.7).

$$\rho = \sqrt{(x - \xi)^2 + (y - \eta)^2 + d^2} \quad (3.7)$$

d is reconstruction distance from hologram plane to reconstruction plane and $(\varepsilon, \eta), (x, y), (\xi, \eta)$ are the co-ordinates in the object plane, hologram plane and reconstruction plane respectively.

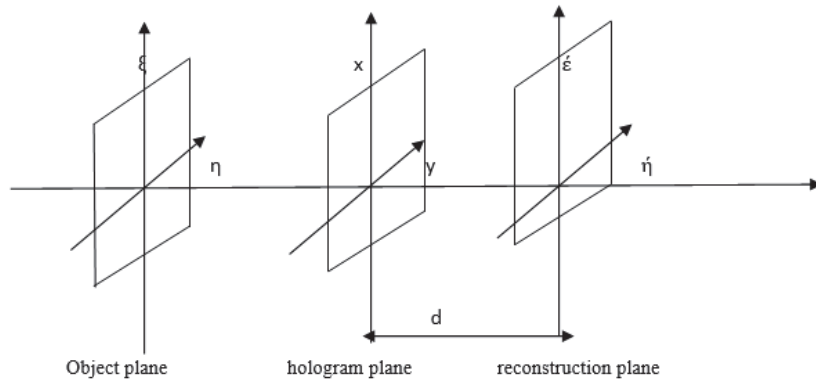


Figure 3-2 Co-ordinate system of hologram formation and reconstruction

According to the Taylor series ρ is approximated as[30],

$$\rho = d + \frac{(x-\xi)^2}{2d} + \frac{(y-\eta)^2}{2d} \quad (3.8)$$

Further the ρ in denominator in equation (3.6) is approximated as d , therefore substitution of equation (3.8) in equation (3.6) gives

$$\Gamma(\xi, \eta) = \frac{i}{\lambda d} \exp(-i \frac{2\pi}{\lambda} d) \iint_{-\infty}^{+\infty} H(x, y) E_R^*(x, y) \exp(-i \frac{\pi}{\lambda d} ((x - \xi)^2 + (y - \eta)^2)) dx dy \quad (3.9)$$

By expanding the term in the exponential will give the equation (3.10)

$$\Gamma(\xi, \eta) = \frac{i}{\lambda d} \exp(-i \frac{2\pi}{\lambda} d) \exp\{-i \frac{\pi}{\lambda d} (\xi^2 + \eta^2)\} \iint_{-\infty}^{+\infty} H(x, y) E_R^*(x, y) \exp\{-i \frac{\pi}{\lambda d} (x^2 + y^2)\} \exp\{i \frac{2\pi}{\lambda d} (x\xi + y\eta)\} dx dy \quad (3.10)$$

This equation is known as Fresnel transformation.

Digital holography use CCD camera to record hologram.

The continuous data is converted to digital form and data is represented in the form of pixels. Let Δx and Δy are pixel sizes in x and y axis respectively. Let $\Delta \xi$ and $\Delta \eta$ are pixel sizes in the reconstruction plane in ξ and η axis respectively. The relation between the pixel sizes in hologram plane and reconstruction plane is given in equation (3.11)

$$\Delta \xi = \frac{\lambda d}{M \Delta x} \quad , \quad \Delta \eta = \frac{\lambda d}{N \Delta y} \quad (3.11)$$

M and N are the number of pixels in x and y axis respectively. Therefore, the reconstruction wave-field in discrete form is obtained by sampling with $\Delta \xi$ and $\Delta \eta$ in ξ and η directions respectively. Thus, $\xi = m\Delta \xi$, $\eta = n\Delta \eta$, $m=0,1,2,3,\dots,M-1$ and $n=0,1,2,3,\dots,N-1$.

Therefore $\Gamma(\xi, \eta) = \Gamma(m\Delta \xi, n\Delta \eta) = \Gamma(m, n)$

$\xi = m\Delta \xi$, $\eta = n\Delta \eta$, equation (3.11) and equation (3.10) together will give rise to equation (3.12)

$$\Gamma(m, n) = \frac{i}{\lambda d} \exp\left(-i \frac{2\pi}{\lambda} d\right) \exp\left\{-i\pi\lambda d \left(\frac{m^2}{M^2\Delta x^2} + \frac{n^2}{N^2\Delta y^2}\right)\right\} \sum_{k=0}^{M-1} \sum_{l=0}^{N-1} E_R^*(k, l) \cdot H(k, l) \exp\left[-i \frac{\pi}{\lambda d} (k^2\Delta x^2 + l^2\Delta y^2)\right] \exp\left[i2\pi\left(\frac{km}{M} + \frac{ln}{N}\right)\right] \quad (3.12)$$

Where $k=0, 1, 2,\dots,M-1$, $l=0, 1, 2,\dots,N-1$.

The above equation written as

$$\Gamma(m, n) = A \cdot \text{DFT} (E_R^*(k, l)) \cdot H(k, l) \exp\left[-i \frac{\pi}{\lambda d} (k^2\Delta x^2 + l^2\Delta y^2)\right] \quad (3.13)$$

Thus the reconstruction wave-field is discrete Fourier transform of the product of the hologram, conjugate of the reference wave and a complex exponential. Further, equation (3.13) can be written as

$$\Gamma(m, n) = A. \mathfrak{F}_\tau ((E_R^* (k, l)) \cdot H(k, l)) \quad (3.14)$$

\mathfrak{F}_τ is an operator known as Fresnel transform.

Thus, the reconstruction wave-field is the Fresnel transform of the product of the hologram and conjugate of reference wave.

3.2.2 Convolution method for reconstruction

This method use convolution theorem for reconstruction of object wave field[30]. We can write the equation (3.6) as

$$\Gamma(\xi, \eta) = \frac{i}{\lambda} \iint_{-\infty}^{+\infty} H(x, y) E_R^* (x, y) g(x, y, \xi, \eta) dx dy \quad (3.15)$$

$$\text{Since } g(x, y, \xi, \eta) = \frac{\exp(-i\frac{2\pi}{\lambda}\rho)}{\rho} \text{ and } \rho = \sqrt{(x - \xi)^2 + (y - \eta)^2 + d^2}$$

$$\text{Therefore } g(x, y, \xi, \eta) = \frac{\exp(-i\frac{2\pi\sqrt{(x-\xi)^2+(y-\eta)^2+d^2}}{\lambda})}{\sqrt{(x-\xi)^2+(y-\eta)^2+d^2}} \quad (3.16)$$

$$\text{Where } g(x, y, \xi, \eta) = g(\xi - x, \eta - y)$$

According to convolution theorem,

$$F_1(\xi, \eta) \Theta F_2(\xi, \eta) = \iint_{-\infty}^{+\infty} F_1(\xi, \eta) \cdot F_2(x - \xi, y - \eta) dx dy$$

Θ means convolution

Hence equation (3.15) can be written as

$$\Gamma(\xi, \eta) = H. E_R^* \Theta g \quad (3.17)$$

Where $H = H(x, y)$, $E_R^* = E_R^* (x, y)$ and $g = g(x, y, \xi, \eta)$

By taking Fourier transform \mathfrak{F} to equation (3.17) gives

$$\mathfrak{F}(\Gamma(\xi, \eta)) = \mathfrak{F}(H. E_R^* \Theta g) = \mathfrak{F}(H. E_R^*) \cdot \mathfrak{F}(g) \quad (3.18)$$

Applying inverse Fourier transform \mathfrak{F}^{-1} to equation (3.18) will give

$$\Gamma(\hat{x}, \hat{y}) = \mathcal{F}^{-1}(\mathcal{F}(H) \cdot E_R^*) \cdot \mathcal{F}(g) \quad (3.19)$$

Thus the wave-field is reconstructed using the convolution algorithm.

3.3 Formulation of reference wave

In digital holography, reconstruction is performed numerically. Once the hologram is recorded, in order to reconstruct object wave-field we have to incident reference beam in optical holography. Similarly in numerical reconstruction as in equation (3.14) and (3.19) are reference wave needs to be defined and it should be the mathematical representation of reference wave that is used for recording the hologram. Any plane wave can be represented as given in equation (3.20)

$$E_R^*(x, y) = \exp[i \frac{2\pi}{\lambda} (k_x x + k_y y)] \quad (3.20)$$

k_x and k_y are the wave vector components in x and y-directions respectively. The direction of propagation of the wave is towards z-axis. Reference wave in discrete form is given in equation (3.21).

$$\text{Reference wave} = R(k, l) = \exp[i \frac{2\pi}{\lambda} (k_x \cdot k \cdot \Delta x + k_y \cdot l \cdot \Delta y)] \quad (3.21)$$

The exact phase reconstruction of the object is obtained only if k_x and k_y are exactly calculated and this reference wave is should match closely to the experimental reference wave [34, 44]. Therefore the reconstruction of object wave-field is Fresnel propagation of product of recorded hologram multiplied by formulated reference wave over reconstruction distance d.

3.4 Zero order diffraction and twin image elimination

We are interested only in the real image, we should eliminate non-diffracted and the twin image (virtual image). The algorithms that used in the in-line holography are different. In in-line holography, all these three terms overlap with each other. In-line holography is known for its simple setup, high resolution of thick volume specimens and insensitive to the instabilities. The main drawback in in-line holography is to eliminate the twin image. Gabor proposed that the twin image problem can be eliminated with two holograms of the object which are reconstructed using quadrature reference waves. Onural et.al[46] and G. Liu et.al[47] explained different algorithms for eliminating the twin image problem. Zero order term should also eliminated to get the real image. This overlap of all the three terms can be eliminated by using off-axis digital holography. In off-axis holography, non-diffracted term, real image and virtual image are spatially

separated. Gu-Liang Chen et.al[48] proposed a method to eliminate the zero order term in which they numerically generated intensities of object and reference waves and subtracted them from digital hologram. Nicolas Pavillon[49] used non-linear filtering for suppression of zero order term in off-axis digital holography, this technique doesn't require a high pass filter which affect the resolution of reconstructed object. Cuhe et.al[50] proposed spatial filtering method for the elimination of zero order and twin image in off-axis digital holography. The Fourier transform of the reconstruction contains three spatial frequency terms corresponding to real image, virtual image and DC term. This zeroth order of diffraction and virtual image is eliminated by selecting only the real image spatial frequency thus eliminating the other two terms.

Thus elimination of zero order of diffraction and the twin image will result in real image reconstruction.

$$\begin{aligned} \text{Reconstruction with spatial filtering} &= E_O^* \cdot |E_R|^2 \\ &= \text{real image} \end{aligned}$$

3.5 Aberration correction

Curvature aberration is produced by using lens because of its geometry. Various methods are developed to compensate aberration as it damages the optical images. J. Upatnieks et.al [51] demonstrated off-axis holography where hologram is spherically aberrated. They used corrector plate to compensate spherical aberration. Then, researchers started working in aberration correction in photographic films where optical aberrations are stored as hologram on the plate and conjugate aberration beam should be send through hologram in such a way to produce collimated beam[52]. Using numerical methods the usage of additional setup for aberration correction is avoided. The use of microscopic objective in DHM will introduce phase curvature. This inherent curvature will cover the exact phase information. For quantitative phase imaging, the curvature correction is necessary. Ferraro et.al[53] proposed different methods to remove the wave-front curvature introduced by the microscopic objective. In one of the method, they extracted phase profile in the area where phase information is not effected by the object and then curvature compensation is performed on whole hologram. In other method, they generated synthetic phase curvature from the fringe pattern in the hologram and phase is corrected at the hologram plane. In other method for structures having flat surface, they proposed the double exposure method. First the hologram is recorded with the microstructure and then the sample is moved transverse to optical axis so that one more hologram of flat surface, microstructure free area is recorded. This 2nd hologram has information of the curvature. That information is used for phase compensation. Colomb et.al[54] proposed automatic procedure to compensate the phase aberrations in DHM. In this method they extract line profiles of reconstructed wave field in and around the sample area where surface is flat. This methods allows curvature correction

introduced by MO, compensation of tilt aberration due to off axis geometry and wave front deformation introduced by the microscopic components. The deformation of the wave front by the MO is shown in Fig 3.3

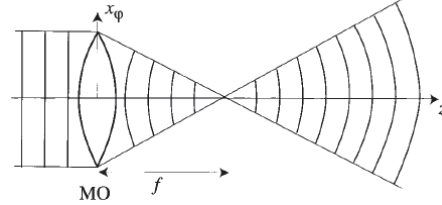


Figure 3-3 Wave front deformation by MO [44]

If we consider the plane wave before the MO in Fig 3.3 as the object wave then we can observe the deformation of wave front introduced by the MO. Digital phase mask(DPM) was defined in [54] to compensate the wave front curvature given in equation (3.22)

$$\Phi(\xi, \eta) = \exp\left[\frac{-i\pi}{\lambda D} (\xi^2 + \eta^2)\right] \quad (3.22)$$

$\Phi(\xi, \eta)$ is DPM, D is radius of curvature which adjusts the curvature of the wave field and negative sign indicates conjugate phase of the curvature produced in objectwave.

Since the DPM is the conjugate of the wave front curvature introduced by the MO. Therefore compensated wave front curvature of the reconstructed wave field is given in equation (3.23)

Reconstructed field with curvature correction=

$$\Gamma_1(\xi, \eta) = \Gamma(\xi, \eta) * \Phi(\xi, \eta) \quad (3.23)$$

$$\text{In discrete form, } \Gamma_1(m, n) = \Gamma(m, n) * \Phi(m, n) \quad (3.24)$$

Using the Fresnel propagation for reconstruction then using equation (3.14) we can write equation (3.24) as

$$\Gamma_1(m, n) = \Phi(m, n) * A \cdot \mathfrak{F}_\tau((E_R^*(k, l)) \cdot H(k, l)) \quad (3.25)$$

It is shown in [54] through the property of Fourier transform equation (3.25) can be written as in equation (3.26)

$$\Gamma_1(m, n) = -i\Phi(m, n) \exp\left(\frac{i2\pi d}{\lambda}\right) E_R^*(m, n) \mathfrak{F}_\tau[H(k, l)] \quad (3.26)$$

DPM and reference wave together can be written as single term as given in equation (3.27)

$$\Gamma_2(\xi, \eta) = \Phi(\xi, \eta) * E_R^*(\xi, \eta) = \exp \left[i \frac{\pi}{\lambda} \left(2k_x \xi + 2k_y \eta - \frac{\xi^2 + \eta^2}{D} \right) \right] \quad (3.27)$$

$$\Gamma_2(m, n) = \Phi(m, n) * E_R^*(m, n) = \exp \left[i \frac{\pi}{\lambda} \left(2k_x (m\Delta\xi) + 2k_y (n\Delta\eta) - \frac{(m\Delta\xi)^2 + (n\Delta\eta)^2}{D} \right) \right] \quad (3.28)$$

Equation (3.28) is the product of DPM and reference wave. But, this equation is limited to 2nd order. In order to compensate for high order errors, generalized polynomial of higher can be defined as given in equation (3.29).

$$\Gamma_2(m, n) = \exp \left[-i \sum_{\alpha=0}^H \sum_{\beta=0}^V P_{\alpha, \beta} (m\Delta\xi)^\alpha (n\Delta\eta)^\beta \right] \quad (3.29)$$

$P_{\alpha, \beta}$ is the polynomial coefficient of order $\alpha + \beta$, H and V represents horizontal and vertical profile order respectively.

$\Gamma_2(m, n)$ Which is the final DPM which contains reference wave information and other higher order correction terms and it can be calculated by taking the horizontal and vertical profiles of the reconstructed wave field and with the help of the curve fitting procedure, phase values of the horizontal and vertical profiles can be mapped to the equation of particular order and polynomial coefficients are calculated and thus final DPM is calculated. The equations for the horizontal and vertical profiles is given by equation (3.30) and (3.31) respectively.

$$Y_h = a_0 + a_1 x + a_2 x^2, \quad \text{where } P_{1,0} = a_1 \& P_{2,0} = a_2 \quad (3.30)$$

$$Y_v = b_0 + b_1 x + b_2 x^2, \quad \text{where } P_{0,1} = b_1 \& P_{0,2} = b_2 \quad (3.31)$$

Thus the polynomial coefficients are calculated, thus final DPM is calculated as given in equation (3.32)

$$\Gamma_2(m, n) = \exp \left[-i (a_1 m + b_1 n + a_2 m^2 + b_2 n^2) \right] \quad (3.32)$$

Thus the final reconstruction of the object is thus given as in equation (3.33)

$$\Gamma_1(m, n) = -i \exp \left(\frac{i2\pi d}{\lambda} \right) * \Gamma_2(m, n) * \mathfrak{F}_\tau [H(k, l)] \quad (3.33)$$

$$\text{Since } \mathfrak{F}_\tau [H(k, l)] = \text{DFT} \{ H(k, l) \exp \left[-i \frac{\pi}{\lambda d} (k^2 \Delta x^2 + l^2 \Delta y^2) \right] \}$$

Equation (3.33) can also be written as

$$\Gamma_1(m, n) = -i \exp\left(\frac{i2\pi d}{\lambda}\right) * \Gamma_2(m, n) * \text{DFT}\{H(k, l) \exp\left[-i \frac{\pi}{\lambda d} (k^2 \Delta x^2 + l^2 \Delta y^2)\right]\} \quad (3.34)$$

Thus equation is final equation for reconstruction of the object wave-field. This procedure should be performed in multiple iterations since initially coefficients are set to zero. The procedure should be continued until polynomial coefficients of last two iterations are approximately same.

Chapter 4

Experiments and results

4.1 Experimental setup

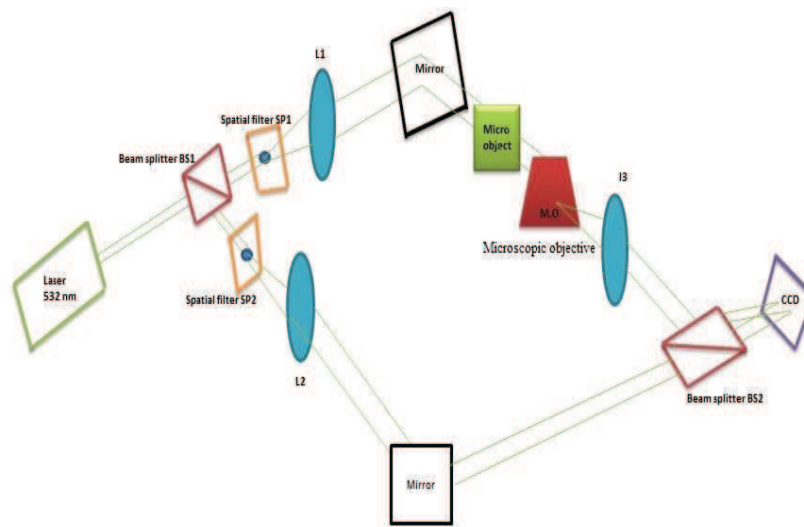


Figure 4-1 Experimental set-up for DHM

The experimental set-up for DHM is given in the Fig 4.1. ‘Nd: YAG’ laser with wavelength 532nm is used. Beam splitter B1 is used to separate the beam into two parts, one is for the object arm and second one is for the reference arm. SP1, SP2 are spatial filters, they are used to remove the random fluctuations from the intensity profile of the beam. L1 and L2 are lenses used for collimating the beam and micro-object is placed in the object arm. Right after the micro-object, Microscopic objective is used to magnify the micro-size object. Lens L3 is used in the object arm to collimate the beam. Beam splitter B2 is used to incident both object beam and reference beam on the CCD camera at an angle Θ . Thus, the two beams interfere on the CCD to record the holograms. The reconstruction of object is done by multiplication of the reference wave with the hologram and propagate wave field to the image plane Fresnel propagation.

4.2 Results

A hologram of object of a letter ‘H’ is cut at the center of an OHP sheet to act as phase object. It is approximately in the order of 1cm*1cm. The recorded hologram is shown in the Fig 4.1

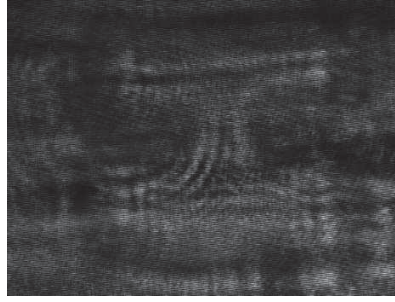


Figure 4-2 Hologram of letter 'H'

The reconstruction of object is carried out using Fresnel propagation as given by the equation (3.13). Reference wave was calculated based on the equation (3.20)

$$E_R^*(x, y) = \exp[i\frac{2\pi}{\lambda}(k_x x + k_y y)]$$

Where $\lambda = 532$ nm, the calculated k_x and k_y are .39961 and 1.600095 respectively

The amplitude reconstruction diffracted image is calculated by taking the modulus of the reconstructed wave-field.

$$\text{Amplitude reconstruction} = |\Gamma(m, n)|$$

Amplitude reconstruction is therefore obtained as shown in the Fig 4.3

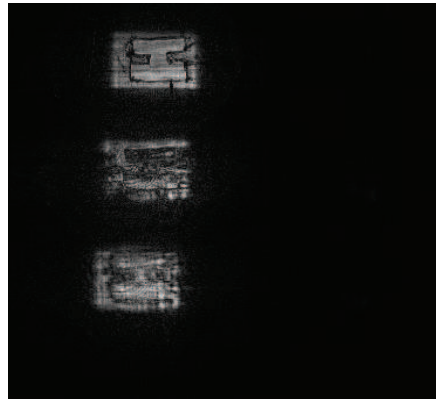


Figure 4-3 Amplitude reconstruction of letter H

The phase reconstruction is obtained from equation (4.1)

$$\text{Phase reconstruction} = \tan^{-1}\left(\frac{\text{img}(\Gamma(m, n))}{\text{real}(\Gamma(m, n))}\right) \quad (4.1)$$

Where $img(\Gamma(m, n))$ and $real(\Gamma(m, n))$ are imaginary and real parts of $\Gamma(m, n)$ respectively.

Thus using equation (4.1) and (3.13) phase reconstruction is shown in the Fig 4.4

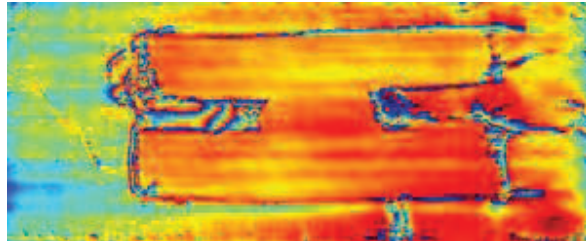


Figure 4-4 Phase reconstruction of letter H

4.2.1 Reconstruction of microscopic phase object

Transparent indium tin oxide (ITO) electrode was used as a micro-object for hologram recording and reconstruction. The concept of ‘synthetic aperture’ is adapted to digital holography’ to improve the resolution and to increase the field of view. The procedure for recording synthetic aperture hologram is explained below.

The concept of synthetic aperture is incorporated from the synthetic aperture radar (SAR) where several individual information (or signal) is combined to form high resolution information. Similarly in this experiment 9 holograms are recorded and all holograms are combined to form a one hologram which contributes to the more information (resolution) of the object and field of view when compared to the single hologram reconstruction. We used CCD camera of pixels 1920 * 2560 and pixel size in x and y directions are given by $\Delta x, \Delta y = 2.2$ micron. If we consider a matrix of size 3*3, where a_{ij} correspond to each of 9 holograms, where $i, j = 1, 2, 3$.

$$\begin{bmatrix} a_{11} & a_{12} & a_{13} \\ a_{21} & a_{22} & a_{23} \\ a_{31} & a_{32} & a_{33} \end{bmatrix}$$

The recording of hologram is started with a_{11} , then the CCD is moved to the right by 1500 pixels using X-Y moving stage. The distance camera move to cross 1500 pixel is 3.3 mm. Thus, the hologram a_{12} is recorded. Similarly, a_{13} is recorded by moving camera to the right by 1500 pixels. Then the CCD is translated down by 1000 pixels which is 2.2mm and hologram a_{23} is recorded. Then it is moved left and so on. Thus, 9 holograms of ITO electrode and the way which we recorded is shown below.

$$\begin{array}{ccccc}
 a_{11} & \rightarrow & a_{12} & \rightarrow & a_{13} \\
 & & & & \downarrow \\
 a_{21} & \leftarrow & a_{22} & \leftarrow & a_{23} \\
 & & \downarrow & & \\
 a_{31} & \rightarrow & a_{32} & \rightarrow & a_{33}
 \end{array}$$

All the recorded holograms of the ITO electrode are shown in the Fig 4.5.

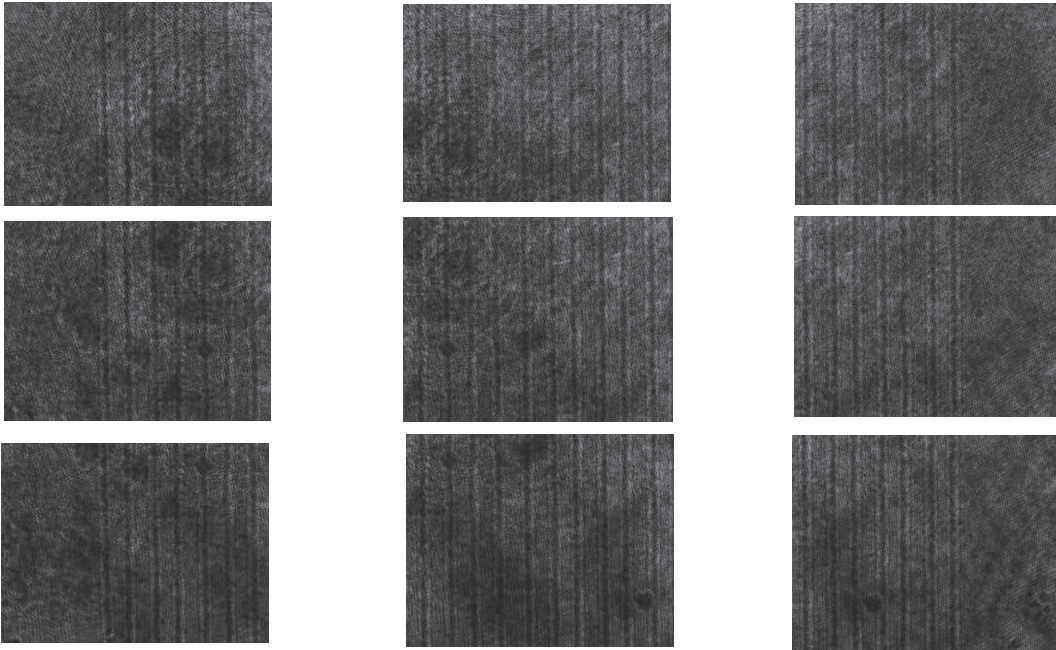


Figure 4-5 Recorded holograms for synthetic aperture reconstruction

All these holograms are stitched together using ‘efficient sub pixel algorithm’[55]. Mosaicked hologram is shown in the Fig 4.6, hologram size is increased, which is similar to increasing the size of CCD by order of 3. The same size of hologram can be recorded if the CCD size of 1920*2560 is replaced with CCD of size of stitched hologram, without moving the CCD.

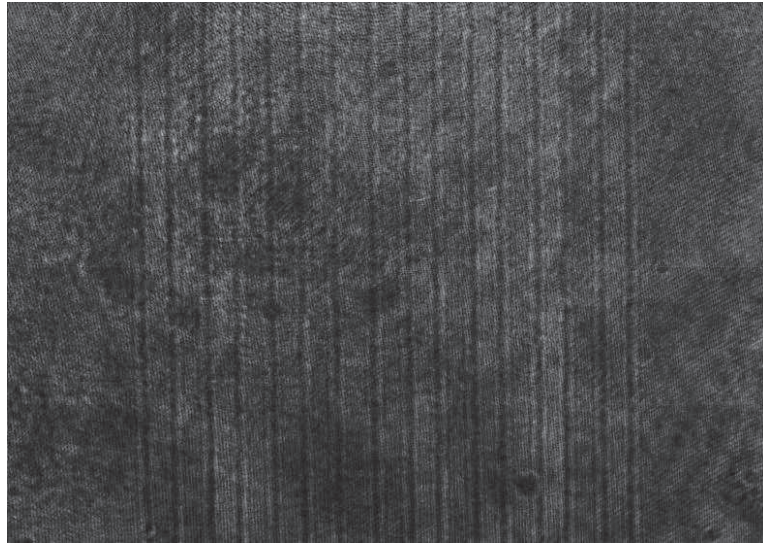


Figure 4-6 mosaicked hologram

The hologram is filtered to avoid twin image and DC term. The Fourier transform of the hologram is taken and three frequency bands correspond to the zero order of diffraction, remaining two are 1st order. The real image spatial frequencies are filtered using butterworth high bandpass filter. The frequency band for single and synthetic aperture hologram is shown in the Fig 4.7 and Fig 4.8 respectively.



Figure 4-7 FFT of single hologram

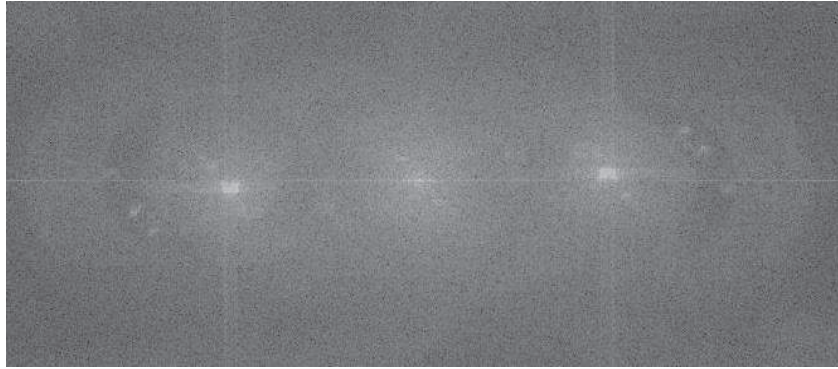


Figure 4-8 FFT of synthetic aperture hologram

The frequency bandwidth in the synthetic hologram is more when compared to single hologram. Only the frequencies which are corresponding to the real image are filtered. Butterworth bandpass pass filter is used. Filtered real image is shown in Fig 4.9.

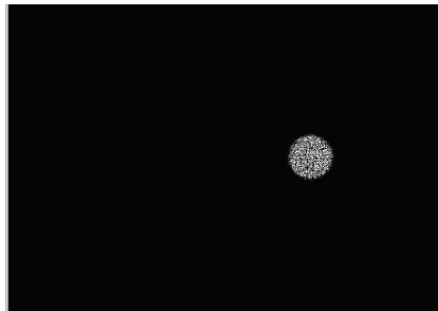


Figure 4-9 Filtered real image

The filtered hologram is used for reconstruction of transparent ITO electrode. We used automatic aberration correction [54] method. The information about reference wave, aberration introduced by MO and other higher order errors are contained in the recorded hologram which is explained in section 3.5. using these information the aberration free phase images can be reconstructed using the Equation (3.34). We have to calculate the DPM for us to calculate the amplitude and phase reconstruction of the object. The wavefront at the image is calculated first the wave front at image plane without DPM. Initialize the reconstruction parameters to $a_1=a_2=b_1=b_2=0$. The reconstructed amplitude and phase images without DPM is shown in Fig 4.10 and Fig 4.11 respectively.

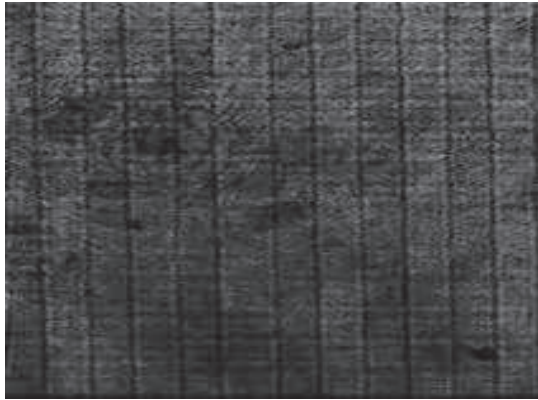


Figure 4-10 Amplitude reconstruction without DPM

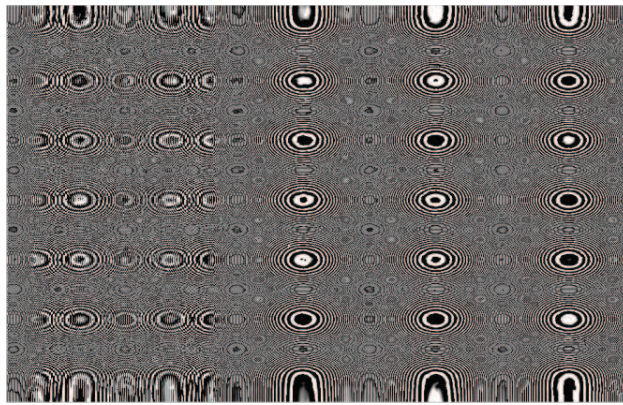


Figure 4-11 Phase reconstruction without DPM

Next step is to extract vertical and horizontal profiles from the phase reconstruction (without DPM). The vertical and horizontal profiles extracted from images shown in the Fig 4.12 and Fig 4.13 respectively.

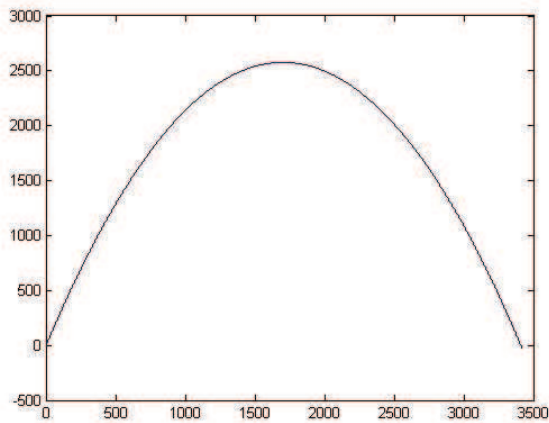


Figure 4-12 Vertical profile

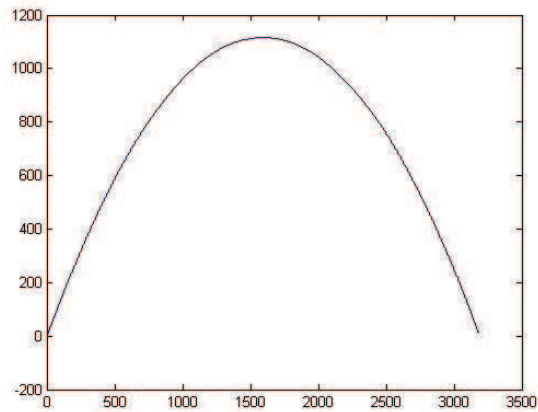


Figure 4-13 Horizontal profile

Using curve fitting analysis, DPM $\Gamma_2(m, n)$ is calculated and it is conjugate of the extracted profiles, so that DPM can cancel out the curvature and other errors in the phase reconstructed image (without DPM). This process should be performed iteratively in order to get exact reconstructed object. The reconstructed ITO electrode using (3.34) is given in Fig 4.15 and it obtained from synthetic aperture hologram. Fig 4.14 shows the ITO electrode from single hologram and Fig 4.15 shows reconstruction of synthetic aperture hologram which is cropped.

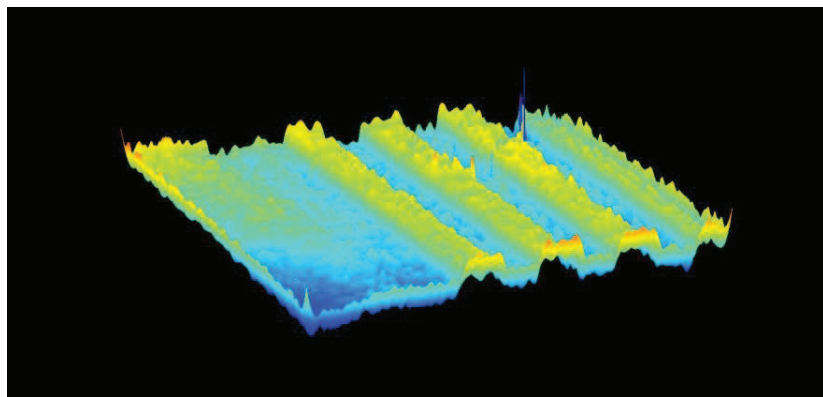


Figure 4-14 Reconstruction of single hologram

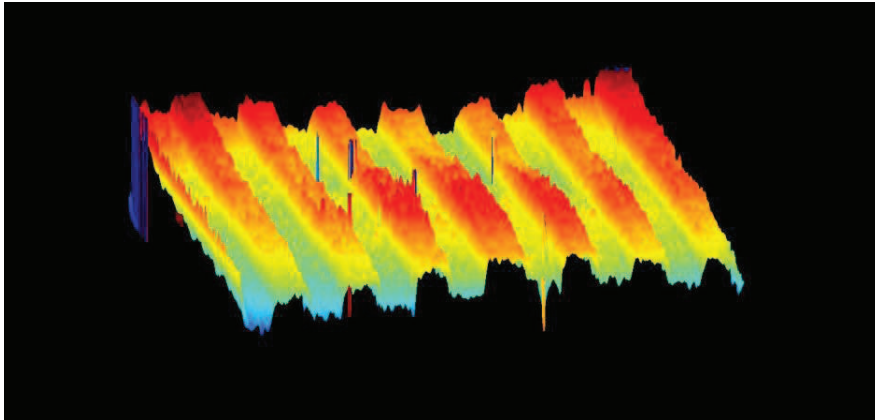


Figure 4-15 Reconstruction of synthetic aperture hologram

We can observe that in synthetic aperture hologram field of view is increased. Thus, we were also able to calculate width and thickness of ITO electrode. The average width of the electrode is around 65-80 μm and the thickness is around 190-300 nm. Thus we were able to characterize ITO electrode and its ability of quantitative phase imaging is shown.

The surface profile can also be calculated by extracting horizontal profile along the reconstructed object and surface profile is shown in the Fig 4.16

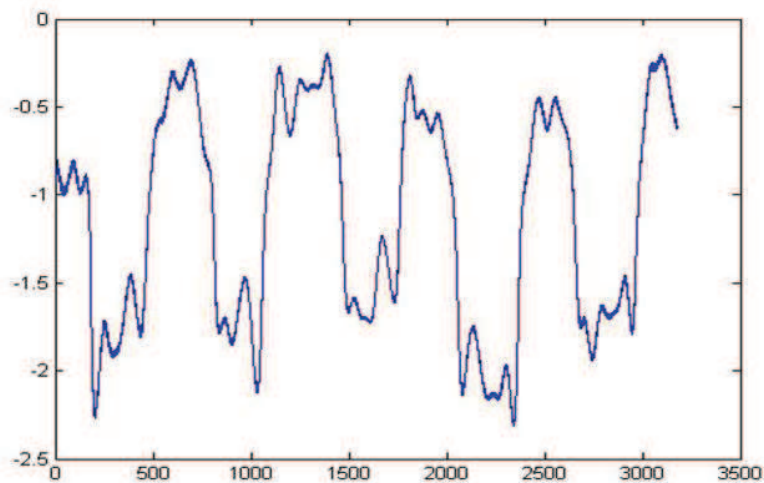


Figure 4-16 Surface plot of ITO electrode using synthetic aperture DHM

In order to show the resolution improvement using SA-DHM we used USAF-resolution chart. The same method for recording synthetic aperture is used of USAF-chart as that of synthetic aperture of ITO electrode. Fig 4.17 and Fig 4.18 shows the amplitude reconstruction of the synthetic aperture USAF chart and single hologram of position a_{22} respectively.

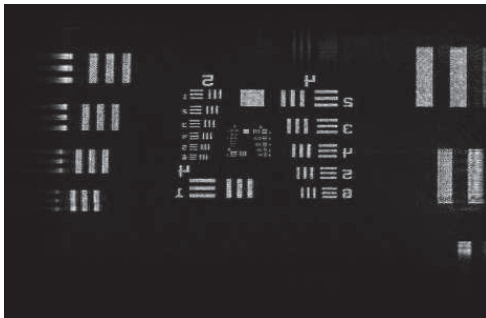


Figure 4-17 Amplitude reconstruction of synthetic aperture of USAF resolution chart

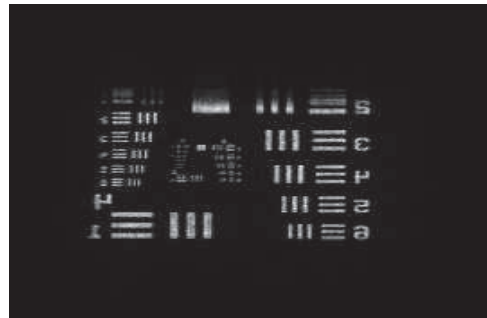


Figure 4-18 Amplitude reconstruction of single hologram of USAF resolution chart

Zoomed version of Fig 4.17 and Fig 4.18 is shown in the figures 4.19 and 4.20, marked region clearly shows improvement of the resolution of SA-DHM.

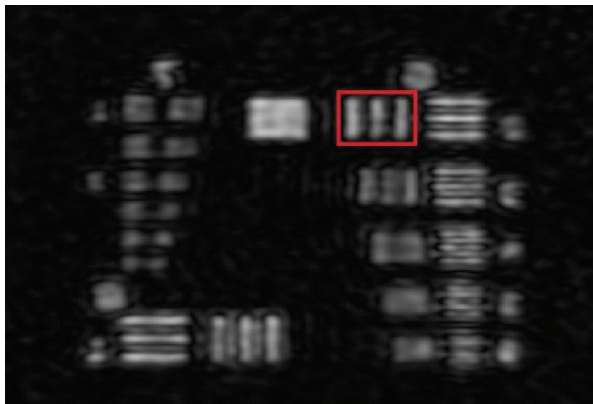


Figure 4-19 Zoomed version of amplitude reconstruction synthetic hologram of USAF resolution chart



Figure 4-20 Zoomed version of amplitude reconstruction single hologram of USAF resolution chart

4.2.2 Reconstruction of cells

Finally, bacterial sample (E.coli) is used for cellular imaging. Fig 4.21 is the phase reconstruction of E.coli for the recorded synthetic hologram and the convolution algorithm is used for reconstruction.

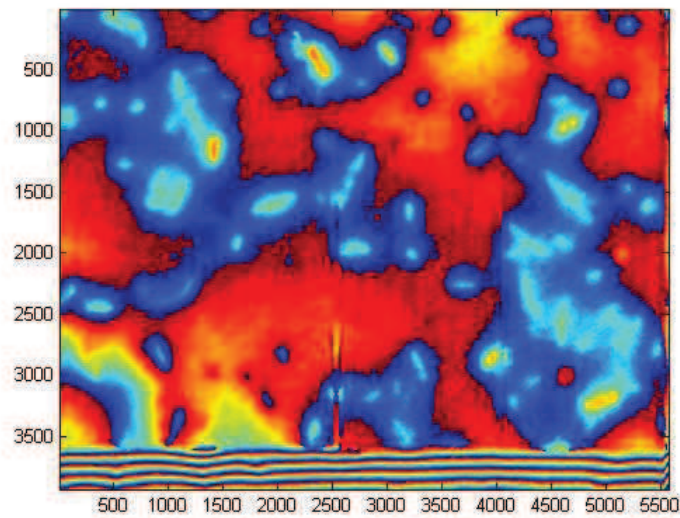


Figure 4-21 Phase reconstruction of E.coli

The individual E.coli is cropped and shown in the Fig 4.22 and Fig 4.23 as 3D rendering

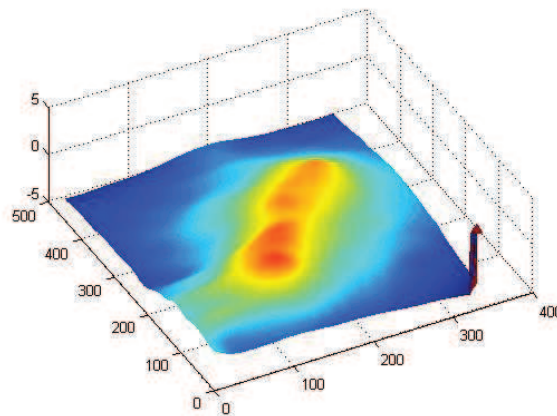


Figure 4-22 Multiplying E.Coli

The length calculated for above Multiplying E.coli is approximately $8\mu\text{m}$ and width is around $2\mu\text{m}$ and the thickness is around $0.1\mu\text{m}$.

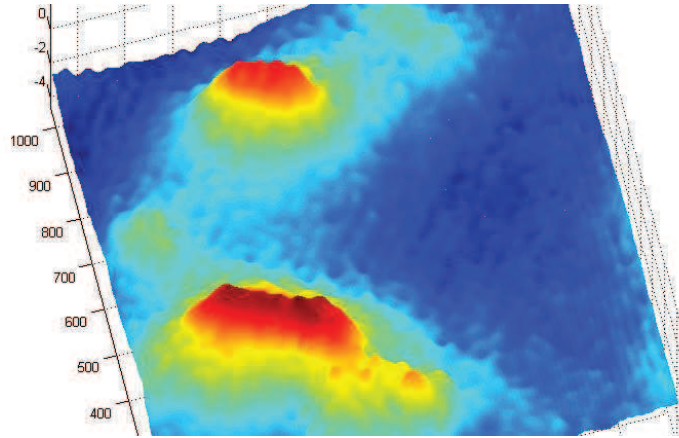


Figure 4-23 E.coli reconstruction

Chapter 5

Summary and future work

Thus DHM is an optical microscopic technique that record the hologram optically and reconstruct the object digitally. Thus, the speed of reconstruction increases and no need to have additional setup for reconstruction as compared to traditional optical holography. DHM is a growing research field with a strong potential for detection of diseases. Various factors like cost, accuracy and speed of reconstruction are actively under development.

We have used SA-DHM for reconstruction of ITO electrode. SA_DHM method is used in order to improve the resolution. We have shown that the transverse resolution can go up to a 100's of nm resolution. We also calculated thickness of the electrode. Thus, quantitative phase imaging ability of DHM is demonstrated. Thus, SA-DHM improves the resolution as well as increase the field of view. We have reconstructed three dimensional structure of E.coli bacteria. Thus, QPI of ITO electrode and bacteria cells are shown.

The advantages of DHM are ability for 3-D imaging, absence of contrast agents, live cell imaging capability, and possibility for multimodal imaging in combination with other optical microscopic techniques.

In Future, work would aim at improving the lateral resolution of the set-up and exploring multimodal imaging techniques along with DHM. . We would extend DHM to live cell imaging to study their dynamics. Efforts are in progress on exploring live cells using lenless-DHM to make low cost and aberration free DHM set-up.

References

1. Massoud, T.F. and S.S. Gambhir, *Molecular imaging in living subjects: seeing fundamental biological processes in a new light*. Genes & development, 2003. **17**(5): p. 545-580.c
2. Vonesch, C., et al., *The colored revolution of bioimaging*. Signal processing magazine, IEEE, 2006. **23**(3): p. 20-31.
3. Thurn, K.T., et al., *Nanoparticles for applications in cellular imaging*. Nanoscale research letters, 2007. **2**(9): p. 430-441.
4. Sun, C., J.S. Lee, and M. Zhang, *Magnetic nanoparticles in MR imaging and drug delivery*. Advanced drug delivery reviews, 2008. **60**(11): p. 1252-1265.
5. Seo, S., et al., *Lensfree holographic imaging for on-chip cytometry and diagnostics*. Lab on a Chip, 2009. **9**(6): p. 777-787.
6. Coskun, A.F., T.-W. Su, and A. Ozcan, *Wide field-of-view lens-free fluorescent imaging on a chip*. Lab on a Chip, 2010. **10**(7): p. 824-827.
7. Zhu, H., et al., *Cost-effective and compact wide-field fluorescent imaging on a cell-phone*. Lab on a Chip, 2011. **11**(2): p. 315-322.
8. Wang, Y.-X.J. and C.K. Ng, *The impact of quantitative imaging in medicine and surgery: Charting our course for the future*. Quantitative imaging in medicine and surgery, 2011. **1**(1): p. 1.
9. Shung, K.K., *Diagnostic Ultrasound: Past, Present, and Future*. Journal of Medical and Biological Engineering, 2011. **31**(6): p. 371-374.
10. Tal Geva, M., *Magnetic Resonance Imaging: Historical Perspective*. Journal of Cardiovascular Magnetic Resonance, 2006. **8**(4): p. 573-580.
11. Sean L Kitson, V.C., Andrea Ciarmiello , Diana Salvo and Luigi Mansi, *Clinical Applications of Positron Emission Tomography (PET) Imaging in Medicine: Oncology, Brain Diseases and Cardiology*. Current Radiopharmaceuticals, 2009. **2**(4): p. 224-253.
12. A. F. Kopp, K.K.-R., M. Heuschmid, A. Küttner, B. Ohnesorge, T. Flohr, S. Schaller, C. D. Claussen, *Multislice Computed Tomography: Basic Principles and Clinical Applications*. electromedica, 2000. **68**(2): p. 94-105.
13. Driss Cammoun, M., Denver; William R. Hendee, PhD, Chicago, and Kathleen A. Davis, MD, Denver, *Clinical Applications of Magnetic Resonance Imaging—Current Status*. West J Med, 1985. **143**(6): p. 793–803.
14. Bilyy, O.I., et al. *Rapid detection of bacterial cells by light scattering method*. in *Biomedical Optics (BiOS) 2008*. 2008. International Society for Optics and Photonics.
15. Francis, L.W., et al., *Atomic force microscopy comes of age*. Biology of the Cell, 2010. **102**(2): p. 133-143.
16. B, M.D., *Fundamentals of light microscopy and electronic imaging*2001: John Wiley & Sons.
17. Abramowitz, M., et al., *Basic principles of microscope objectives*. Biotechniques, 2002. **33**(4): p. 772-781.
18. Young, M.R., *Principles and Technique of Fluorescence Microscopy*. Quarterly Journal of Microscopical Science, 1961. **102**(4): p. 419-449.
19. Petty, H.R., *Fluorescence microscopy: established and emerging methods, experimental strategies, and applications in immunology*. Microscopy research and technique, 2007. **70**(8): p. 687-709.

20. Ikeda, T., et al., *Hilbert phase microscopy for investigating fast dynamics in transparent systems*. Optics letters, 2005. **30**(10): p. 1165-1167.
21. Popescu, G., et al., *Erythrocyte structure and dynamics quantified by Hilbert phase microscopy*. Journal of biomedical optics, 2005. **10**(6): p. 060503-060503-3.
22. Rockward, W.S., et al., *Quantitative phase measurements using optical quadrature microscopy*. Applied Optics, 2008. **47**(10): p. 1684-1696.
23. Warger, W.C., et al., *Multimodal optical microscope for detecting viability of mouse embryos in vitro*. Journal of biomedical optics, 2007. **12**(4): p. 044006-044006-7.
24. Popescu, G., et al., *Fourier phase microscopy for investigation of biological structures and dynamics*. Optics letters, 2004. **29**(21): p. 2503-2505.
25. Park, Y., et al., *Diffraction phase and fluorescence microscopy*. Optics express, 2006. **14**(18): p. 8263-8268.
26. Bhaduri, B., et al., *Diffraction phase microscopy: principles and applications in materials and life sciences*. Advances in Optics and Photonics, 2014. **6**(1): p. 57-119.
27. Bhaduri, B., et al., *Diffraction phase microscopy with white light*. Optics letters, 2012. **37**(6): p. 1094-1096.
28. Ding, H. and G. Popescu, *Instantaneous spatial light interference microscopy*. Optics express, 2010. **18**(2): p. 1569-1575.
29. Hariharan, P., *Optical Holography: Principles, techniques and applications* 1996: Cambridge University Press.
30. Schnars, U. and W. Jueptner, *Digital holography* 2005: Springer.
31. Brown, B.R. and A.W. Lohmann, *Complex spatial filtering with binary masks*. Applied Optics, 1966. **5**(6): p. 967-969.
32. Goodman, J.W. and R.W. Lawrence, *Digital image formation from electronically detected holograms*. Applied Physics Letters, 1967. **11**(3): p. 77-79.
33. Schnars, U. and W. Jüptner, *Direct recording of holograms by a CCD target and numerical reconstruction*. Applied Optics, 1994. **33**(2): p. 179-181.
34. Cuche, E., F. Bevilacqua, and C. Depeursinge, *Digital holography for quantitative phase-contrast imaging*. Optics letters, 1999. **24**(5): p. 291-293.
35. Pedrini, G., Y.L. Zou, and H.J. Tiziani, *Simultaneous quantitative evaluation of in-plane and out-of-plane deformations by use of a multidirectional spatial carrier*. Applied Optics, 1997. **36**(4): p. 786-792.
36. Schnars, U. and W.P. Jüptner, *Digital recording and reconstruction of holograms in hologram interferometry and shearography*. Applied Optics, 1994. **33**(20): p. 4373-4377.
37. Schnars, U., *Direct phase determination in hologram interferometry with use of digitally recorded holograms*. JOSA A, 1994. **11**(7): p. 2011-2015.
38. Yamaguchi, I. and T. Zhang, *Phase-shifting digital holography*. Optics letters, 1997. **22**(16): p. 1268-1270.
39. Lai, S., B. King, and M.A. Neifeld, *Wave front reconstruction by means of phase-shifting digital in-line holography*. Optics communications, 2000. **173**(1): p. 155-160.
40. Yamaguchi, I., J.-i. Kato, and S. Ohta, *Surface shape measurement by phase-shifting digital holography*. Optical review, 2001. **8**(2): p. 85-89.
41. Yamaguchi, I., T. Matsumura, and J.-i. Kato, *Phase-shifting color digital holography*. Optics letters, 2002. **27**(13): p. 1108-1110.
42. Javidi, B. and T. Nomura, *Securing information by use of digital holography*. Optics letters, 2000. **25**(1): p. 28-30.

43. Lee, K., et al., *Quantitative phase imaging techniques for the study of cell pathophysiology: from principles to applications*. Sensors, 2013. **13**(4): p. 4170-4191.
44. CuChe, E., P. Marquet, and C. Depeursinge, *Simultaneous amplitude-contrast and quantitative phase-contrast microscopy by numerical reconstruction of Fresnel off-axis holograms*. Applied Optics, 1999. **38**(34): p. 6994-7001.
45. Gabor, D., *Nobel Lecture, December 11, 1971*.
46. Onural, L. and P. Scott, *Digital decoding of in-line holograms for imaging fractal aggregates*. Electronics Letters, 1986. **22**(21): p. 1118-1119.
47. Liu, G. and P. Scott, *Phase retrieval and twin-image elimination for in-line Fresnel holograms*. JOSA A, 1987. **4**(1): p. 159-165.
48. Chen, G.-L., et al., *Numerical suppression of zero-order image in digital holography*. Optics express, 2007. **15**(14): p. 8851-8856.
49. Pavillon, N., et al., *Suppression of the zero-order term in off-axis digital holography through nonlinear filtering*. Applied Optics, 2009. **48**(34): p. H186-H195.
50. CuChe, E., P. Marquet, and C. Depeursinge, *Spatial filtering for zero-order and twin-image elimination in digital off-axis holography*. Applied Optics, 2000. **39**(23): p. 4070-4075.
51. Upatnieks, J., A.V. Lugt, and E. Leith, *Correction of lens aberrations by means of holograms*. Applied Optics, 1966. **5**(4): p. 589-593.
52. DeHainaut, C., et al., *Holographic correction of aberrations using PLZT*. Applied Optics, 1988. **27**(16): p. 3551-3555.
53. Ferraro, P., et al., *Compensation of the inherent wave front curvature in digital holographic coherent microscopy for quantitative phase-contrast imaging*. Applied Optics, 2003. **42**(11): p. 1938-1946.
54. Colomb, T., et al., *Automatic procedure for aberration compensation in digital holographic microscopy and applications to specimen shape compensation*. Applied Optics, 2006. **45**(5): p. 851-863.
55. Guizar-Sicairos, M., S.T. Thurman, and J.R. Fienup, *Efficient subpixel image registration algorithms*. Optics letters, 2008. **33**(2): p. 156-158.